

COMPUTER-AIDED FREE VIBRATION ANALYSIS OF GUYED TOWERS

by

Giovanni Militano
B.Sc. (Civil Engineering)

A Thesis

Submitted to the Faculty of Graduate Studies
in Partial Fulfillment of the Requirements
for the Degree of

Master of Science

Department of Civil and Geological Engineering
University of Manitoba
Winnipeg, Manitoba
© June, 2000



**National Library
of Canada**

**Acquisitions and
Bibliographic Services**

395 Wellington Street
Ottawa ON K1A 0N4
Canada

**Bibliothèque nationale
du Canada**

**Acquisitions et
services bibliographiques**

395, rue Wellington
Ottawa ON K1A 0N4
Canada

Your file *Votre référence*

Our file *Notre référence*

The author has granted a non-exclusive licence allowing the National Library of Canada to reproduce, loan, distribute or sell copies of this thesis in microform, paper or electronic formats.

The author retains ownership of the copyright in this thesis. Neither the thesis nor substantial extracts from it may be printed or otherwise reproduced without the author's permission.

L'auteur a accordé une licence non exclusive permettant à la Bibliothèque nationale du Canada de reproduire, prêter, distribuer ou vendre des copies de cette thèse sous la forme de microfiche/film, de reproduction sur papier ou sur format électronique.

L'auteur conserve la propriété du droit d'auteur qui protège cette thèse. Ni la thèse ni des extraits substantiels de celle-ci ne doivent être imprimés ou autrement reproduits sans son autorisation.

0-612-53192-9

Canada

**THE UNIVERSITY OF MANITOBA
FACULTY OF GRADUATE STUDIES

COPYRIGHT PERMISSION PAGE**

Computer-Aided Free Vibration Analysis of Guyed Towers

BY

Giovanni Militano

**A Thesis/Practicum submitted to the Faculty of Graduate Studies of The University
of Manitoba in partial fulfillment of the requirements of the degree
of
M.SC**

GIOVANNI MILITANO © 2000

Permission has been granted to the Library of The University of Manitoba to lend or sell copies of this thesis/practicum, to the National Library of Canada to microfilm this thesis/practicum and to lend or sell copies of the film, and to Dissertations Abstracts International to publish an abstract of this thesis/practicum.

The author reserves other publication rights, and neither this thesis/practicum nor extensive extracts from it may be printed or otherwise reproduced without the author's written permission.

ABSTRACT

Guyed towers are used for communication purposes and are frequently designed to heights of 300 meters (1000 feet). A guyed tower is a non-linear structure in which the mast, typically consisting of multiple truss members is supported laterally at several points by inclined guy cables. The guy cables are anchored to a foundation and are pre-tensioned. Wind induced vibrations may result in a fatigue failure of a guy anchor linkage or a cable, ultimately causing the collapse of an entire tower. In addition, excessive deflections or vibrations may interfere with communications and control systems resulting in serviceability failure. According to design standards, a basic understanding of the dynamic characteristics of guyed towers is important. This study develops an easy to use software package, aimed at practicing engineers, to determine free-vibration characteristics (natural frequencies and mode shapes) of guyed towers. The analysis presented herein employs the finite element method to determine the natural frequencies and mode shapes of guyed towers. The structural system is broken down into two main components, the tower mast and guy cables. Utilizing an equivalent beam-column analysis that takes into consideration different lacing patterns, the mast is modelled as a beam-column with equivalent properties. A three-dimensional cable finite element following a catenary or parabolic profile is used to model guy cables. Several comparisons are made to ensure the accuracy of the cable element and the guyed tower model. Selected numerical results are presented for natural frequencies and mode shapes of a few representative towers. The influence of cable tension, lacing pattern of the mast and configuration of guy cables is also examined. The software package can be extended to include forced vibration response through the modal superposition method.

ACKNOWLEDGEMENTS

The author would like to express his appreciation for the time, advice and guidance that Dr. R.K.N.D Rajapakse contributed towards the completion of the present study. Without his interest and support, the present study would never have been undertaken nor completed. The author would also like to thank Mr. Ben Yue from Manitoba Hydro who provided valuable advice and data. The author's appreciation is also extended to the examination panel of Mr. Ben Yue and Dr. Q. Zhang for their review of the thesis and comments.

Financial assistance was provided by Manitoba Hydro. Without this financial support the author would not have been able to undertake graduate studies and as such is most thankful to Manitoba Hydro.

Finally, the author would like to extend a special thank you to his parents and friends for their continuous support and encouragement.

TABLE OF CONTENTS

Abstract	ii
Acknowledgements	iii
Table of Contents	iv
List of Tables	vii
List of Figures	viii
Chapter 1: Introduction	1
1.1 General.....	1
1.2 Literature Review.....	2
1.3 Scope and Objectives.....	6
Chapter 2: Structural Dynamics Model	9
2.1 General Description of Structural Model.....	9
2.2 Guy Cable Element.....	10
Equivalent Modulus of Elasticity	11
Cable Profile.....	11
Cable Element Stiffness	13
Cable Element Mass	16
2.3 Tower Mast Element.....	17
Axial Load and Self Weight Effects.....	20
2.4 Torsion Arm Model	20
Microwave Satellite Dishes.....	22
2.5 Free Vibration Analysis	23
Chapter 3: Natural Frequencies of Cables and Beams	25
3.1 Comparison of Cable Frequencies.....	25
Tightly Stretched Cable	25
Horizontal Cable.....	26
Inclined Cable.....	29

3.2 Comparison of Beam Frequencies	32
Torsional Vibrations	33
Flexural Vibrations	34
Axial Vibrations	34
3.3 Equivalent Beam-Column Representation.....	35
Chapter 4: Software Development	39
4.1 Graphical User Interface (GUI)	39
4.2 Pre-Processor and Post-Processor.....	41
4.3 Finite Element Engine (FEE).....	42
4.4 Software Installation	43
Installation Requirements	43
Installing GTAP.....	44
4.5 Software Instructions and Model Development.....	44
Chapter 5: Free Vibration Characteristics of Guyed Towers	53
5.1 WTMJ Tower.....	53
Natural Frequencies	53
Mode Shapes.....	58
5.2 Parametric Study.....	61
Tower Mast Lacing Patterns	61
Guy Cable Tension	67
Chapter 6: Conclusions	71
References	74
Nomenclature	78
Appendix	79
Three-Dimensional Cable Element.....	79

Three-Dimensional Beam Element	81
Star Mount (Torque Frame)	85
Three Meter Outrigger	85
Eight Foot Outrigger	86
Twelve Foot Outrigger	87
WTMJ Tower Properties	88

LIST OF TABLES

Table 2.1	Equivalent beam-column properties	19
Table 3.1	In-plane symmetric modes for a horizontal sagging cable	28
Table 3.2	In-plane anti-symmetric modes for a horizontal sagging cable	28
Table 3.3	Out-of-plane modes for a horizontal sagging cable	29
Table 3.4	Chord inclination effects.....	30
Table 3.5	Comparison of catenary and elasticity solutions	32
Table 3.6	Comparison of torsional vibration frequencies	33
Table 3.7	Comparison of flexural vibration frequencies	34
Table 3.8	Comparison of axial vibration frequencies	35
Table 3.9	Comparison of flexural vibration frequencies	38
Table 5.1	Natural frequencies of WTMJ guy cables.....	54
Table 5.2	Natural frequencies of tower mast neglecting cable interaction	55
Table 5.3	WTMJ natural frequencies (out-of-plane stiffness included)	57
Table 5.4	WTMJ natural frequencies (out-of-plane stiffness neglected).....	58
Table 5.5	Material properties of Towers A and B	61
Table 5.6	Natural frequencies of Tower A for various lacing patterns.....	65
Table 5.7	Natural frequencies of Tower B for various lacing patterns	65
Table 5.8	Natural frequencies of Tower A for variations in cable tension.....	69
Table A.1	Guy Properties – WTMJ Tower.....	87
Table A.2	Tower Mast Properties – WTMJ Tower	89

LIST OF FIGURES

Figure 1.1	Cross section of a typical mast.....	2
Figure 2.1	Finite element idealization of a typical guyed tower	10
Figure 2.2	Inclined guy cable with parabolic profile	12
Figure 2.3	Inclined guy cable with catenary profile.....	13
Figure 2.4	Three dimensional cable element.....	14
Figure 2.5	Tower segment.....	18
Figure 2.6	Tower lacing patterns.....	18
Figure 2.7	Space truss	19
Figure 2.8	Torsion arm.....	21
Figure 2.9	Guy configuration for tower with torsion arms	22
Figure 2.10	Microwave satellite dishes.....	22
Figure 2.11	Dynamic equilibrium of a spring-mass-dashpot system.....	23
Figure 3.1	Horizontal sagging cable.....	26
Figure 3.2	Variation of natural frequency with Sag ratio for a horizontal cable.....	30
Figure 3.3	Variation of natural frequency with sag ratio for a cable inclined at 30°.....	31
Figure 3.4	Variation of natural frequency with sag ratio for a cable inclined at 60°.....	31
Figure 3.5	Latticed tower segment	36
Figure 3.6	Latticed tower mast.....	37
Figure 4.1	General program interaction	40
Figure 4.2	FEE program interaction.....	43
Figure 4.3	Main GTAP window.....	45
Figure 4.4	Project Information window	46
Figure 4.5	Tower Base window	46
Figure 4.6	Tower Information window	47
Figure 4.7	Tower Sections window.....	48
Figure 4.8	Elements window.....	49

Figure 4.9	Guy + Guy Rings window	50
Figure 4.10	Guy Rings window	50
Figure 4.11	Guy Cable window	51
Figure 4.12	Post Processor window	52
Figure 4.13	Post Processor – animated modeshapes	52
Figure 5.1	WTMJ tower modeshapes.....	61
Figure 5.2	Geometry of Tower A.....	63
Figure 5.3	Geometry of Tower B	64
Figure 5.4	Select modeshapes of Tower A.....	66
Figure 5.5	Select modeshapes of Tower B.....	67
Figure 5.6	Tower A subject to sustained uniform wind loading.....	68
Figure A.1	Plane of a cable	81
Figure A.2	Notation for a three-dimensional beam element.....	82
Figure A.3	Three meter outrigger.....	86
Figure A.4	Eight foot outrigger.....	86

Chapter 1

INTRODUCTION

1.1 GENERAL

Guyed towers are almost exclusively used for communication purposes and structural reliability of guyed communication towers is becoming an important factor in the ever-increasing demand for wireless communication technologies. Guyed towers are frequently designed to heights of 300 meters (1000 feet) and are used to transmit and receive high frequency signals for various electronic communication systems including those associated with electric power distribution. Slender masts laterally supported by pre-tensioned guy cables are typically adopted for this purpose as they provide an economical solution compared to self-supporting latticed towers.

A guyed tower is generally a non-linear structure in which the mast, typically consisting of multiple truss members and of triangular or square cross section (Figure 1.1), is supported laterally at several points by inclined guy cables. The cables are attached to buried concrete anchors and are pretensioned. The non-linearity is primarily associated with structural behaviour of guy cables and that may significantly complicate the analysis of the entire structure. Typical guy cables comprise of galvanized bridge strand in accordance with ASTM Standard A586. Guy diameters normally range between 20 and 50 mm (3/4" to 2").

Guyed towers used for communication purposes must be designed to meet stringent deflection requirements. This is necessary since a minor misalignment of

satellite dishes mounted on the tower may result in loss of communication signals, which could lead to disruptions or poor quality service to thousands of customers. Wind induced vibrations are the primary source for excessive tower deflections. Therefore, the dynamic response of guyed towers is an important aspect in the design of towers for communication purposes. In addition, wind induced vibrations occurring over an extended period of time may induce fatigue failures in various elements of a guyed tower. A better understanding of the dynamic behaviour of guyed towers is also important to facilitate design against fatigue failure. In seismic zones, guyed towers must be designed to withstand earthquake loads. Public utilities or federal agencies own nearly all guyed towers built in Canada.

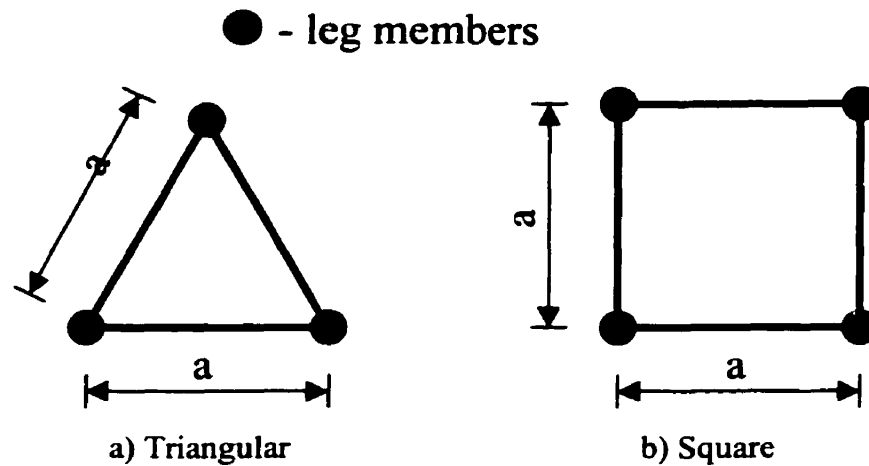


Figure 1.1: Cross section of a typical mast.

1.2 LITERATURE REVIEW

Many researchers have studied static and dynamic behaviour of guyed towers. A simple way to analyze a guyed tower is to assume the mast of the structure to be a continuous beam on elastic supports with a set of springs to idealize the taut guy cables attached to the tower mast. An obvious improvement to this simple model would be to consider the sag in guy cables.

Cohen and Perrin (1957a and 1957b) made the earliest contributions to the study of guyed towers. Their first paper (1957a) investigated wind loading and presented a set of charts that could be used to predict the drag loads produced by wind on various types

of structures. The second paper (1957b) presented a model that described the behaviour of a guyed tower. The mast was treated as a cantilever beam-column on elastic supports and the guy cables were considered to follow a parabolic profile. Rowe (1958) investigated the amplification of stresses and displacements in guyed towers when changes in geometry are included. Modelling the guys as bars, charts were developed that could be used to determine when advanced methods of structural analysis are required in the design and what modifications could be made to the analysis to obtain reasonable results.

Hull (1962) expressed the critical moment of inertia corresponding to a critical buckling wind load and conducted a stability analysis of guyed towers. It was suggested that increasing the stiffness of guys is the most efficient means of increasing the buckling capacity of a tower. It was shown that the buckling capacity could be increased up to the limit where it begins to buckle into a number of sine waves. Hull showed that once this point has been reached, a further increase of guy stiffness does not increase the buckling load of a tower. At this stage, it was found that the only way to further increase the buckling capacity of a tower was to increase the moment of inertia of mast.

Goldberg and Myers (1965) investigated the importance of including wind effects on guy cables. A method of analysis was presented for guyed towers that considered non-linear behaviour and the effect of wind on guy cable stiffness. The study also reported that neglecting wind effects on guy cables resulted in discrepancies in the end moments, shear, guy tensions and lateral displacements. Following the assumption that an inclined guy cable follows a parabolic profile, Odley (1966) presented a solution where secondary effects (ice loads, shear deformations, etc.) were included in the guyed tower model. The analysis was carried out by assuming a value for the deflection of the mast at each guy level, which is used to determine the moments and reactions. Using these reactions, deflections were determined analytically and compared with the assumed deflections. This trial and error procedure was repeated until all assumed and computed values of deflection fall within a predetermined tolerance.

Williamson and Margolin (1966) showed the importance of including shear effects in the analysis of guyed towers. They presented a method for modifying the conventional moment distribution factors when the axial thrust and web flexibility of a

tower is included. In the analysis, the shaft was replaced by a fictitious solid web that had an equivalent shear rigidity of a flexible trussed web. To account for shear deformations, modified moment distribution constants were presented. Miklofsky and Abegg (1966) presented a simplified systematic procedure for the design of guyed towers by use of interaction diagrams. A tower is first analyzed following the assumption that it is a continuous beam on elastic supports while secondary effects are included. The tower is then re-analyzed including amplification stresses from axial loads. The interaction diagrams provided a designer with a graphical visualization of the design range thereby preventing a trial and error procedure.

Goldberg and Gaunt (1973) presented a method that could be used to determine the instability of guyed towers. In their analysis, lateral load increments are applied until a tower reaches instability. The criterion used to define buckling in the analysis is the occurrence of a large increase in the tower deformations for a small increase in the applied load. A parametric study was also included which showed the influence of certain system parameters on the critical load of a tower. They showed that increasing the moment of inertia of the shaft was a less effective way of increasing the critical load.

Based on the assumption that the static profile of a cable followed the shape of a parabola, Davenport (1959) presented a dynamic guy modulus which was meant to take into account the effects of the dynamic nature of wind loading on a guy and a mast. Dean (1961) introduced catenary equations for the static profile of a guy cable. Dean argued that due to the availability of computers there is no need to use a parabolic approximation in the analysis of a cable. Dean also continued on to present his derivation of a dynamic guy modulus. However, Davenport among others (Dean 1962) found fault that Dean's derivation neglected to include elastic stretch of a cable. Following up previous work by Davenport (1959) and again assuming a parabolic approximation for the static profile of a guy cable, Davenport and Steels (1965) considered the effects of aerodynamic damping and transverse vibrations.

Using catenary equations, O'Brian (1967) presented an iterative numerical procedure for the solution of a sagging cable. This iterative procedure presented an important step in the development of a better cable element. In one of the first studies to consider the extensional characteristics of a cable, Irvine and Caughey (1974) presented a

linear theory for the free-vibration of a uniform horizontally suspended cable for ratios of sag-to-span of 1:8 or less. They showed that if the sag is small enough for the static geometry to be described by a parabola, the theory provided good results. These authors also developed expressions for the natural frequencies of a horizontal cable fixed at both ends for in-plane and out-of-plane motions. The expressions were presented as functions of the cables axial stiffness, horizontal tension, self-weight and cable effective length. In addition to a horizontal cable, consideration was also given to the analysis of inclined cables. The effects of inextensible cable assumption were also discussed.

West et al. (1975) considered elastic effects and used straight bars connected by frictionless pins to derive the fully non-linear equations of motion for free vibrations and a linearized version of it. The solution resulted in frequencies and modes associated with small oscillations about the equilibrium configuration. However, the work reported was limited to in-plane motions and horizontal cables only. Henghold and Russell (1976) and Henghold et al. (1977) made additional improvements to the analysis of an elastic guy cable. These authors employed the finite element method to develop a three-node geometrically non-linear cable element and considered three-dimensional free vibrations of an extensible cable hanging under self-weight. Extending an analytical approach, Irvine (1978) presented solutions for free vibrations of an inclined cable hanging under self-weight. Non-dimensional natural frequencies of symmetric in-plane modes were shown to depend only on one dimensionless system parameter while the remaining frequencies were shown to be independent of any parameters. Analytical expressions were presented in a form that could be used to reproduce the results obtained by Henghold et al. (1977).

By using an equivalent modulus of elasticity, Fleming (1979) used the finite element method to model non-linear behaviour of cables. Ekhande and Madugula (1988) later adopted this concept of an equivalent modulus of elasticity in their study. Following a parabolic profile of an inclined cable, Veletsos and Darbre (1983) presented a linearized approximation of the equations of motion for an inclined cable. Using these equations, the dynamic stiffness of a cable could be derived. This approach produced results similar to those of Irvine (1981), but could also accommodate for large inclinations of the cable.

In many studies, guyed towers have been assumed to oscillate linearly about their static equilibrium position. This allowed for the use of a "Modal Approach" (McCaffrey 1969, McCaffrey and Hartmann 1972, and Novak et. al. 1978) for dynamic analysis. The above studies assumed a mast as an equivalent beam-column and a lumped mass idealization. Saxena (1988) considered the free vibration of complex guyed towers. The cable element used in the study was based on the formulation of Veletsos and Darbre (1983). Stiffness of the mast was evaluated in an approximate manner by considering only leg members. As a consequence, the lacing pattern of a tower has no influence on the response. More recently, Kahla (1993) presented an equivalent beam-column analysis. The study introduced equivalent beam-column properties for several square and triangular lacing patterns. The coupling between different degrees of freedom was addressed by the use of a geometric coupling matrix.

1.3 SCOPE AND OBJECTIVES

Field inspections in Manitoba and other provinces have identified a number of problems associated with guyed tower members. These problems have included excessive vibration of tower members and guy cables and structural failure at the guy anchors. Examination of some problematic guy anchors revealed that the anchors had failed in a brittle manner. A brittle failure typically indicates a fatigue problem induced by cyclic loading conditions. Wind induced vibrations in guy cables may subject guy anchor linkages or the guy cable to cyclic loading conditions. Over time these conditions can lead to fatigue failure at the anchor or the guy cable, both of which could cause the collapse of a tower. In addition, excessive deflections due to wind induced vibrations can cause towers to misalign and cause an interference with communication and control systems.

During the early and late winter months freezing rain is not an uncommon occurrence throughout the Prairie Provinces. Freezing rain when combined with wind can create undesirable effects on guy cables. During storms, rain (driven by wind) can freeze on the guy cables and form what resembles an aerodynamic wing. The wind passing around this newly formed wing may then pick up and drop the cable. The

repeated occurrence of this phenomenon is known as galloping. Galloping can cause failure of a guy or guy linkage and may lead to the collapse of a tower.

The Canadian Standard CSA-S37-M94 states that guyed towers should be serviceable and safe from collapse. The tower should also be of sufficient rigidity such that the serviceability limits of twist or tilt are not exceeded. The standard also mentions that guyed towers are susceptible to dynamic excitation due to wind turbulence. It is recommended (but not mandatory) that a dynamic analysis be conducted and that it should include all significant vibration modes and account for structural and aerodynamic damping of mast and guys. The standard also briefly describes a method to determine the dynamic response of a tower referred to as the Patch Load Method. Using this method, steady and fluctuating components of guyed tower response are calculated separately and then combined to obtain peak design response.

Manitoba Hydro currently owns and manages several guyed towers in the province. These towers are used to communicate streams of data from generating stations and are also used by telecommunication companies for various cellular services. In an effort to provide practicing engineers with a better understanding of the basic structural dynamic characteristics of a guyed tower, this study presents a user friendly computer-aided software package for free vibration analysis of guyed towers.

As such, the present study seeks to provide an efficient method for free vibration analysis of guyed towers. This is accomplished by considering the three main components of a guyed tower. Namely, the guy cables, the tower mast and torsion arms. As part of the study, a new three-dimensional cable element is developed. Existing methods of analysis are utilized to represent the tower mast as a three-dimensional beam. Furthermore, a stiffness and mass matrix representation is developed for some common torsion arm configurations. By using the finite element method (FEM), the above tower components are integrated into a model to represent a guyed tower and a free-vibration analysis is completed. The above tasks are completed utilizing a computer algorithm developed in this study. Furthermore, an interactive and easy to use graphical user interface (GUI) is developed as part of the software package. The graphical interface serves as a front and back end to the computer algorithm.

The theory and structural model that constitute the basis of the finite element analysis are described in Chapter 2. The structural model is based largely on an equivalent beam-column model for mast, equivalent truss element for torsion arms and sagging cables following parabolic or catenary profiles. To verify the validity of stiffness and mass representations of the mast and cables, several comparisons are made in Chapter 3 with exact analytical and existing numerical solutions. Chapter 4 discusses the development, layout, and provides user instructions for the software package developed in this study. The basic dynamic behaviour of representative multi-level guyed towers is examined in Chapter 5. A set of conclusions is given in Chapter 6. The finite element program developed in this study is broad and expandable, and has been developed as a user-friendly tool for practising engineers. Options are available for cable representation (parabolic and catenary) and tower lacing patterns. The software package can be expanded to include forced vibration analysis through the modal superposition method.

Chapter 2

STRUCTURAL DYNAMICS MODEL

2.1 GENERAL DESCRIPTION OF STRUCTURAL MODEL

The selection of a mathematical model to simulate the response of a structure is a very important step in any analysis. Assumptions made at this point determine if the developed model reasonably represents the actual behavior of the structure under consideration. In the present study, the finite element method (FEM) was used to model the guy cables and mast of a guyed tower system. The FEM involves dividing a structure into a discrete number of elements from which an approximate numerical solution is obtained. With the ease of programming the FEM on personal computers, this approach provides an efficient means for developing an accurate solution for many structural analysis problems.

A finite element idealization of a typical guyed tower is shown in Figure 2.1. As can be seen from the figure, the model consists of two main components, cable and mast elements. The elements are inter-connected to one another by the nodes, each of which may have as many as six degrees of freedom (DOF). The choice of structural elements used to model a system and the number of elements used in an analysis could have a significant impact on the accuracy as well as the computational efficiency of the solution.

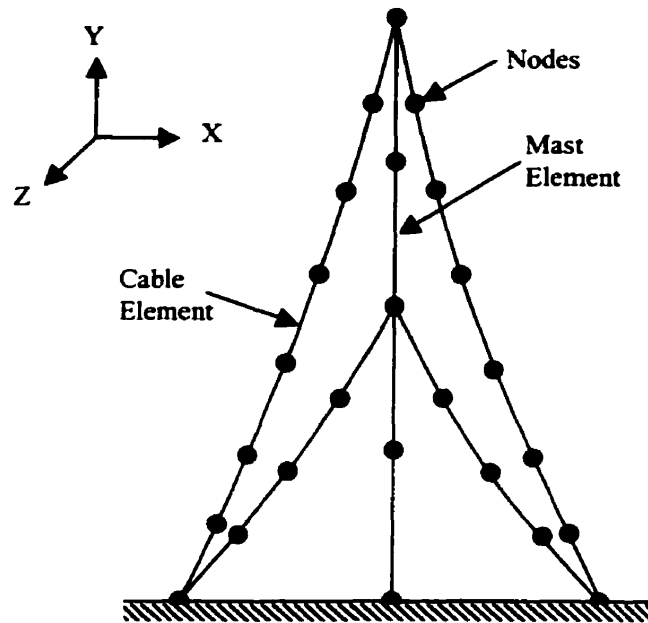


Figure 2.1: Finite element idealization of a typical guyed tower.

In this study, a three-dimensional beam-column model was used to represent the mast of the tower. The beam column model consists of six DOF at each node. The guy cables were represented by a three-dimensional cable element with three DOF at each node. Star mounts (cross arms) are modeled by equivalent truss elements, while satellite dishes as lumped masses with negligible stiffness. Once the guyed tower has been discretized into elements, the individual mass and stiffness matrices of each element are computed. By employing the standard assembly procedure (Harrison, 1973) the mass and stiffness matrices of the entire structure are determined. The global mass and stiffness matrices are then used to determine the free vibration frequencies and modeshapes of the structure.

2.2 GUY CABLE ELEMENT

Guy cables are commonly used to support freestanding towers that may extend to greater heights. These guyed structures are generally elastic in nature, but non-linear in their geometric sense. This non-linear behavior is a result of the non-linear axial force-

deformation relationship for due to the sag caused by their own self-weight. The non-linear behavior of a guyed tower complicates the analysis of the structure significantly. To accurately model a guy cable, a three-dimensional inclined cable element with parabolic or catenary profile was used in the present study. The application of an equivalent modulus of elasticity for a guy cable based on straight cord assumption was also examined.

EQUIVALENT MODULUS OF ELASTICITY

A conventional method to account for the non-linearity due to sag of an inclined guy cable has been to consider an equivalent straight chord member while the modulus of elasticity is modified and represented by an equivalent modulus of elasticity. This equivalent modulus of elasticity (E_{eq}) considers both the effects of material and geometric deformations (Fleming 1979). The equivalent modulus of elasticity may be represented as

$$E_{eq} = \frac{E_c}{\left[1 + \left(\frac{w^2 L_p^2 A_c E_c}{12T^3} \right) \right]} \quad (2.1)$$

where E_{eq} is the equivalent modulus of elasticity for the cable, E_c is the modulus of elasticity for the cable, L_p is the projected length of a cable on a plane normal to the direction gravity, w is the unit weight of the cable, A_c is the cross-sectional area of the cable and T is the tension in the cable.

CABLE PROFILE

Many past studies (Davenport 1959, Irvine and Caughey 1974, Veletsos and Darbre 1983) have used the assumption that the static profile of a sagging cable subjected to its own weight and an externally applied axial tensile force may be represented by a parabolic profile. In the case of a guy cable being used to support a tower, the high pretension force may often cause the sag of the guy cable to be relatively small. Under these circumstances, Irvine (1981) argued that the parabola provides a reasonable approximation of the static profile of a sagging cable provided that the sag-to-span ratio is less than 1:8.

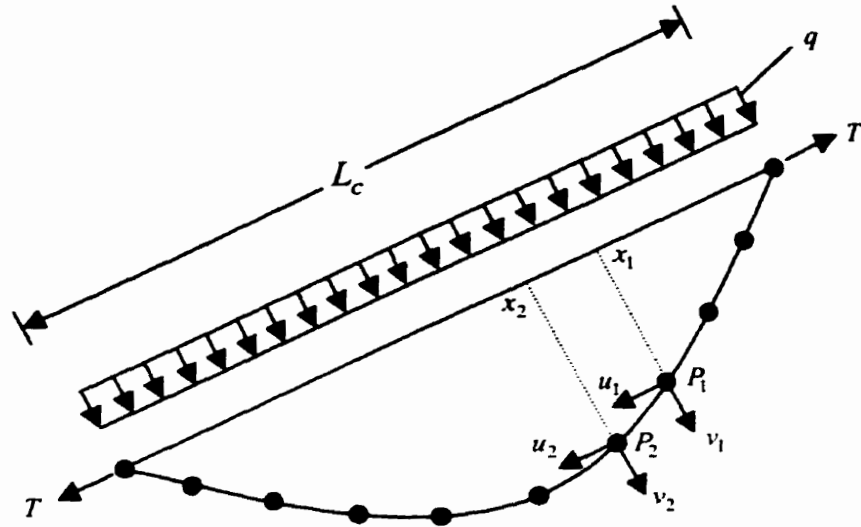


Figure 2.2: Inclined guy cable with parabolic profile.

With reference to the co-ordinate system shown in Figure 2.2, the deflection of an inclined sagging cable subject to an externally applied tension was given by (Veletsos and Darbre 1983)

$$y(x) = \frac{1}{2} \frac{qL_c^2}{T} \left(\frac{x}{L_c} - \left(\frac{x}{L_c} \right)^2 \right). \quad (2.2)$$

In many existing analyses (Davenport 1959, Irvine 1981, etc.) of guys and guyed structures, the profile of a sagging guy cable has been assumed to follow the shape of a parabola. However, this simplifying assumption can introduce errors in the cable profile and subsequently in the natural frequencies obtained from an analysis. Such errors can be quite small in some cases, such as the case of a tightly stretched cable where the sag is small. If however the chord is not horizontal, then symmetry is lost and the parabolic approximation can introduce significant errors (Dean 1961). Since the catenary profile has been considered to provide the best approximation for a sagging cable, the catenary equation developed by Dean (1961) was adopted in the present study for the static equilibrium profile of a guy cable.

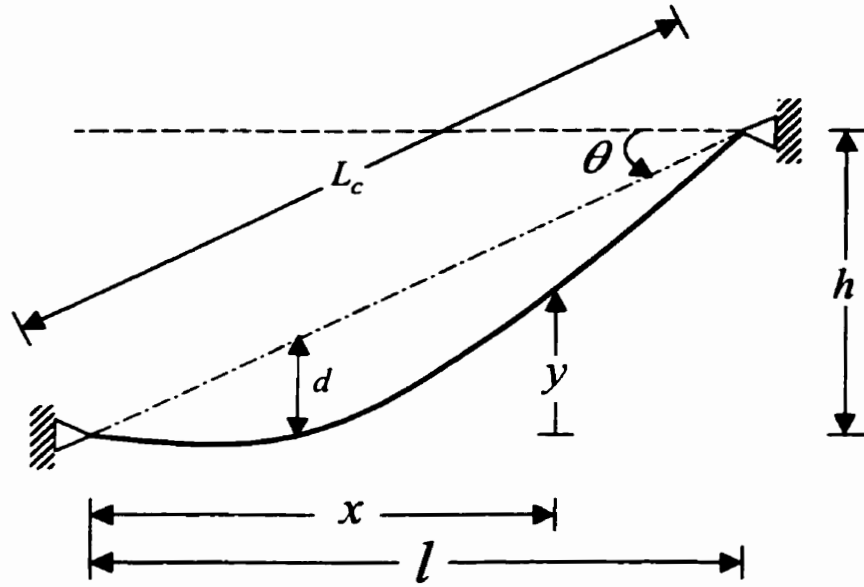


Figure 2.3: Inclined guy cable with catenary profile.

Consider the guy cable shown in Figure 2.3. The profile of the cable may be described by (Dean 1961)

$$y = \frac{H}{q} \cosh\left(\frac{q}{H}x + a_1\right) + a_2 \quad (2.3)$$

where H is the horizontal component of the cable tension, q is the distributed self weight of the cable and

$$a_1 = \sinh^{-1}\left[\frac{qh}{2H \sinh(ql/2H)}\right] - \frac{ql}{2H}; \quad a_2 = -\frac{H}{q} \cosh a_1. \quad (2.4)$$

The tension at any point on the cable is given by

$$T = H \cosh\left(\frac{q}{H}x + a_1\right). \quad (2.5)$$

CABLE ELEMENT STIFFNESS

For a cable structure such as a guyed tower, the displacements are not very large and the geometry of the system is well defined prior to an analysis. The dynamic behavior is usually low frequency responses due to wind excitation. For these cable structures, it has been common to model the guy cables by using a series of short truss links and non-linear computer codes developed for solid structures (Peyrot and Goulois 1979). It has been shown that an inclined cable supported at its ends and subjected to its

own weight and an externally applied tensile force follows a catenary profile (Dean 1961 and Irvine 1981). The axial stiffness of the cable varies with a change in sag, which in turn varies with the displacement of the cable ends. Hence for cable elements, the sag must be considered if an accurate analysis is to be obtained (Fleming 1979).

Figure 2.4 shows a typical cable element of length L_c , cross-sectional area A_c , and mass density ρ . By employing the concepts of conventional finite element method, the stiffness matrix of the inclined cable element shown in Figure 2.4 can be developed. Let u_i , v_i , and w_i be the end displacements of the cable element along the positive x , y , and z directions respectively so that there are three degrees of freedom at each node. The displacements u , v and w at an arbitrary point on the cable element shown in Figure 2.4 is interpolated as (Zienkiewicz and Taylor 1989)

$$u = \sum_{i=1}^2 N_i u_i, \quad v = \sum_{i=1}^2 N_i v_i, \quad w = \sum_{i=1}^2 N_i w_i \quad (2.6)$$

where N_i is the shape function at node i defined by

$$N_1 = \frac{1}{2}(1 - \xi); \quad N_2 = \frac{1}{2}(1 + \xi). \quad (2.7)$$

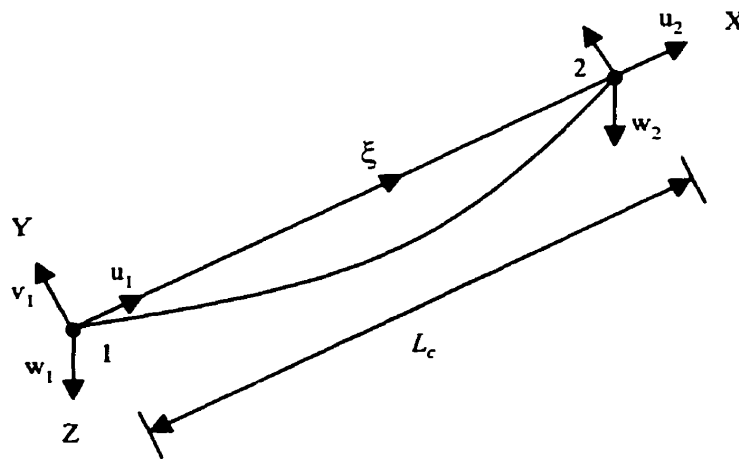


Figure 2.4: Three-dimensional cable element.

Cartesian co-ordinates along the cable element is given by (Zienkiewicz and Taylor 1989)

$$x = \sum N_i x_i, \quad y = \sum N_i y_i, \quad z = \sum N_i z_i. \quad (2.8)$$

The relationship between Cartesian and curvilinear co-ordinate system is given by $|J|$ where

$$|J| = \frac{\partial x}{\partial \xi}. \quad (2.9)$$

The strain-displacement relationship for an axial member is given by (Zienkiewicz and Taylor, 1989)

$$\varepsilon_x = (\varepsilon_x)_L + (\varepsilon_x)_{NL} \quad (2.10)$$

where

$$(\varepsilon_x)_L = \text{Linear strain} = \frac{\partial u}{\partial x} \quad (2.11)$$

$$(\varepsilon_x)_{NL} = \text{Non-linear strain} = \frac{1}{2} \left\{ \left(\frac{\partial u}{\partial x} \right)^2 + \left(\frac{\partial v}{\partial x} \right)^2 + \left(\frac{\partial w}{\partial x} \right)^2 \right\} \quad (2.12)$$

$$(\varepsilon_x)_L = \frac{du}{dx} = \frac{du}{d\xi} \frac{d\xi}{dx} = \frac{1}{|J|} \frac{du}{d\xi} = [B_L] \{d\} \quad (2.13)$$

where $[B_L]$ is the linear strain matrix for a cable element and $\{d\} = \{u_1, u_2\}^T$ and

$$(\varepsilon_x)_{NL} = \frac{1}{2} \left\{ \frac{\partial u}{\partial x}, \frac{\partial v}{\partial y}, \frac{\partial w}{\partial z} \right\} \begin{Bmatrix} \frac{\partial u}{\partial x} \\ \frac{\partial v}{\partial y} \\ \frac{\partial w}{\partial z} \end{Bmatrix}. \quad (2.14)$$

Let us define

$$[G] \{\delta\} = \begin{Bmatrix} \frac{\partial u}{\partial x} \\ \frac{\partial v}{\partial y} \\ \frac{\partial w}{\partial z} \end{Bmatrix} \quad (2.15)$$

where $\{\delta\} = \{u_1, v_1, w_1, u_2, v_2, w_2\}^T$ and $[G]$ is the gradient matrix defined by

$$[G] = \begin{bmatrix} \frac{\partial N_1}{\partial x} & 0 & 0 & \frac{\partial N_2}{\partial x} & 0 & 0 \\ 0 & \frac{\partial N_1}{\partial x} & 0 & 0 & \frac{\partial N_2}{\partial x} & 0 \\ 0 & 0 & \frac{\partial N_1}{\partial x} & 0 & 0 & \frac{\partial N_2}{\partial x} \end{bmatrix}. \quad (2.16)$$

The strain energy U of a cable element is given below.

$$\begin{aligned}
U &= \frac{1}{2} \int_V \{\varepsilon_x\}_L^T \{\sigma\} dV + \int_V \{\varepsilon_x\}_{NL}^T \{\sigma_0\} dV \\
&= \frac{1}{2} \int_V \{\varepsilon_x\}_L^T E \{\varepsilon_x\} dV + \int_V \{\varepsilon_x\}_{NL}^T \sigma_0 dA dx \\
&= \frac{E_c A_c}{2} \int_{-1}^1 \{d\}^T [B_L]^T [B_L] \{d\} |J| d\xi + \frac{T_0}{2} \int_{-1}^1 \{\delta\}^T [G]^T [G] \{\delta\} |J| d\xi \\
&= \frac{1}{2} \{d\}^T [K_E] \{d\} + \frac{1}{2} \{\delta\}^T [K_G] \{\delta\}
\end{aligned} \tag{2.17}$$

where σ_0 is the initial stress, and T_0 is the pre-tension force

$$T_0 = \sigma_0 \int dA = \sigma_0 A. \tag{2.18}$$

Based on equation 2.10, the elastic stiffness matrix $[K_E]$ of the cable element is expressed as

$$[K_E]_{(2 \times 2)} = EA \int_{-1}^1 [B_L]^T [B_L] |J| d\xi \tag{2.19}$$

and the geometric stiffness matrix $[K_G]$ is expressed as

$$[K_G]_{(6 \times 6)} = T_0 \int_{-1}^1 [G]^T [G] |J| d\xi. \tag{2.20}$$

CABLE ELEMENT MASS

The lumped-mass representation is the simplest mathematical model for inertia forces of structural elements. In this idealization, masses are lumped at the node points with respect to the translational and rotational inertia of an element. The lumped masses are determined on the assumption that the material within the mean locations on either side of the specified node behaves like a rigid body while the remainder of the element does not participate in such motion. This assumption does not include the dynamic coupling between element displacements, and the resulting mass matrix is purely diagonal (Przemieniecki 1968). The lumped-mass matrix of the cable element shown in Figure 2.4 is given by

$$[m] = \frac{\rho A_c L_e}{2} \begin{bmatrix} 1 & 0 & 0 & 0 & 0 & 0 \\ 0 & 1 & 0 & 0 & 0 & 0 \\ 0 & 0 & 1 & 0 & 0 & 0 \\ 0 & 0 & 0 & 1 & 0 & 0 \\ 0 & 0 & 0 & 0 & 1 & 0 \\ 0 & 0 & 0 & 0 & 0 & 1 \end{bmatrix} \tag{2.21}$$

where ρ is the mass density, L_e is the effective cable length and A_c is the cable area.

However, the solution accuracy based on lumped-mass representation is not as good as if a consistent-mass is used (Przemieniecki 1968 and Logan 1992). The lumped-mass representation has the advantage that the matrix is diagonal and the numerical operations for the solution of the dynamic equilibrium equations are in most instances reduced substantially (Bathe 1982).

Based on variational principles, a mass matrix consistent with the displacement interpolation functions can be derived. It can be shown that the consistent mass matrix of a cable element of volume V can be expressed as

$$[m] = \iiint_V \rho [N]^T [N] dV. \quad (2.22)$$

By evaluating the above integral, the consistent-mass matrix of the cable element shown in Figure 2.4 is found to be

$$[m] = \frac{\rho A_c L_e}{6} \begin{bmatrix} 2 & 0 & 0 & 1 & 0 & 0 \\ 0 & 2 & 0 & 0 & 1 & 0 \\ 0 & 0 & 2 & 0 & 0 & 1 \\ 1 & 0 & 0 & 2 & 0 & 0 \\ 0 & 1 & 0 & 0 & 2 & 0 \\ 0 & 0 & 1 & 0 & 0 & 2 \end{bmatrix}. \quad (2.23)$$

The present study considered both lumped-mass and consistent-mass approaches in the modeling.

2.3 TOWER MAST ELEMENT

A proper structural model of the mast is necessary in order to ensure that accurate results are obtained for a guyed tower system. The mast, which consists of multiple truss members, can be represented as a beam-column of equivalent stiffness based on the properties and geometry of the mast.

By using the unit load method to determine the displacements of the centroidal axis of a mast for various loads, the equivalent beam-column properties were derived by Kahla (1993). This approximate method of analysis provides a simple and efficient way to analyze guyed towers. Figure 2.5 shows a space truss and its equivalent beam-column model. For the five lacing patterns shown in Figure 2.6, Kahla (1993) determined the

equivalent beam-column properties for a mast of triangular cross-section. These equivalent properties are shown in Table 2.1.

In Table 2.1, EA is the equivalent axial stiffness, EI_x and EI_z are the equivalent flexural stiffness in the x and the z directions, GA_x and GA_z are the equivalent shear stiffness in the x and z directions and GJ is the equivalent torsional stiffness. The remaining properties are defined in Figure 2.7 where A_h , A_d and A_t are the areas of the vertical, diagonal and horizontal truss members. The space truss shown in Figure 2.7 represents a typical segment of a triangular lacing pattern as shown in Figure 2.6.

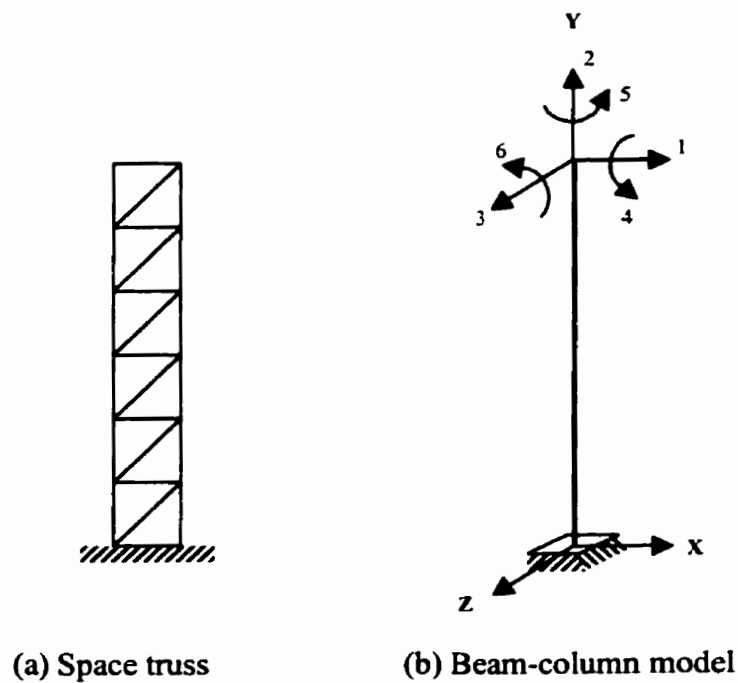
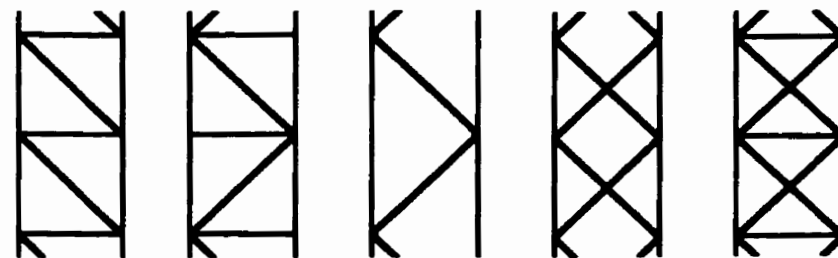


Figure 2.5: Tower segment.



a) Pattern 1 b) Pattern 2 c) Pattern 3 d) Pattern 4 e) Pattern 5

Figure 2.6: Tower lacing patterns.

Equivalent Property	Pattern 1	Pattern 2 and 3
EA	$3EA_h$	$3EA_h$
EI_x, EI_z	$EA_h a^2 / 2$	$EA_h a^2 / 2$
GA_x, GA_z	$1 / \left(\frac{2}{3EA_d \sin^2 \theta \cos \theta} + \frac{2 \tan \theta}{3EA_s} \right)$	$3EA_d \sin^2 \theta \cos \theta / 2$
GJ	$1 / \left(\frac{4}{Ea^2} \left(\frac{1}{A_h \tan^2 \theta} + \frac{1}{A_d \sin^2 \theta \cos \theta} + \frac{\tan \theta}{A_s} \right) \right)$	$1 / \left(\frac{4}{Ea^2} \left(\frac{1}{A_h \tan^2 \theta} + \frac{1}{A_d \sin^2 \theta \cos \theta} \right) \right)$
Equivalent Property	Pattern 4	Pattern 5
EA	$3EA_h$	$3E \left(A_h + \frac{A_s A_d \cos^3 \theta}{A_s + 2A_d \sin^3 \theta} \right)$
EI_x, EI_z	$EA_h a^2 / 2$	$\frac{Ea^2}{2} \left(A_h + \frac{A_s A_d \cos^3 \theta}{2(A_s + 2A_d \sin^3 \theta)} \right)$
GA_x, GA_z	$3EA_d \sin^2 \theta \cos \theta$	$3EA_d \sin^2 \theta \cos \theta$
GJ	$Ea^2 A_d \sin^2 \theta \cos \theta / 2$	$Ea^2 A_d \sin^2 \theta \cos \theta / 2$

Table 2.1: Equivalent beam-column properties.

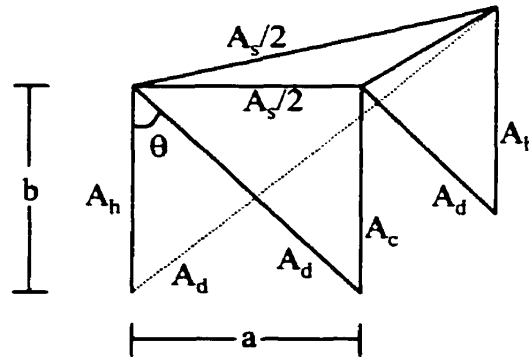


Figure 2.7: Space truss.

Based on the equivalent beam-column properties presented above, the stiffness and mass representation of the three-dimensional beam-column model can be obtained. The stiffness and mass matrices for a slender three-dimensional frame element (beam-column) which considers axial, transverse and bending motion is given by Craig (1981).

However, this stiffness and mass representation does not consider shear deformation and rotatory inertia effects. Stiffness and mass representations for a three-dimensional beam element which considers shear effects is given by Przemieniecki (1968). The stiffness and mass matrix representations given by Craig and Przemieniecki are presented in the Appendix for completeness.

AXIAL LOAD AND SELF WEIGHT EFFECTS

Guyed towers often extend to heights of 100 meters or more. As a result, self-weight of the tower can exert a considerable axial load on the lower portions of the tower mast. The basic beam stiffness matrix does not include the effects of a compressive axial load or the effects of element self weight. An axial load on a beam element can have a significant effect on its dynamic behavior (Przemieniecki 1968). The effect of tower self weight was taken into consideration by incorporating the geometric and axial load stiffness matrices with the basic stiffness matrix of a beam. Complete geometric and axial load stiffness matrices are presented in the Appendix.

2.4 TORSION ARM MODEL

The upper level guys are often attached to the tower mast by triangular star mounts often referred to as torsion arms. These arms are primarily used to reduce twisting of a tower in an effort to keep microwave satellite dishes in alignment so as to limit any disruptions to communication signals. The typical configuration of a torsion arm is shown in Figure 2.8(a).

A torsion arm typically consists of short non-symmetrical slender lattice members. Since the members are slender, shear deformations can be safely ignored (Timoshenko 1960). A star mount cannot be modelled as a rigid member or as a series of equivalent beams which connect a guy cable to the equivalent beam-column representing the mast since this would not account for tension of a cable on mast. Instead, the torsion arm was modelled as a space truss. The stiffness matrix was derived by considering the degrees of freedom (DOF) at the cable end and the point of attachment of the star mount with the mast. One end of the mount is connected to the legs of the mast at four points

(Figure 2.8). Deformations on this plane were assumed to remain planar due to considerably higher stiffness of tower mast in comparison to that of star mount. Subsequently, a star mount was modelled as having three translations and three rotations at the point of contact with the beam-column, while the free end to which the cable is attached has only three translations. This results in a 9×9 stiffness matrix that was computed by conducting a series of truss analyses. These analyses were carried out using the software package SAP90™. The mass matrix was formed by a traditional lumped mass technique. The star mount's structural mass and stiffness matrices are presented in Appendix A.

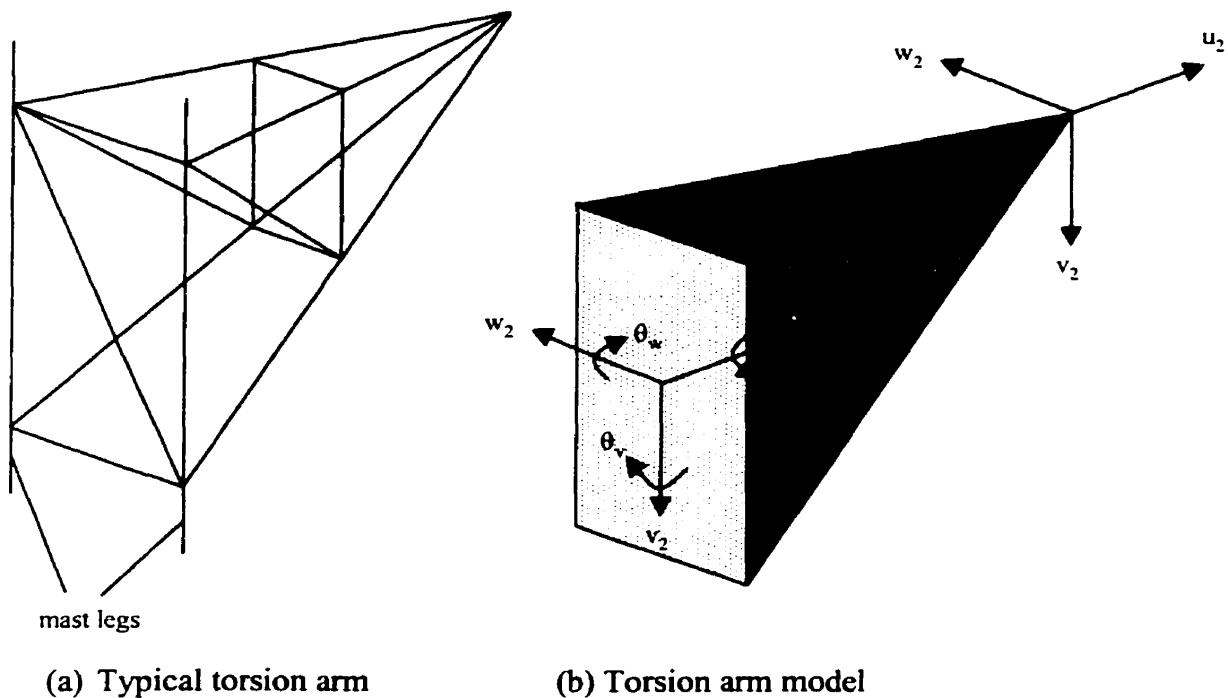


Figure 2.8: Torsion arm.

The pre-processor developed in this study provides a user with a few standard torsion arms to choose and the option of employing one of the two common cable configurations shown in Figure 2.8. Dimensions and sections properties of some standard torsion arms are included in the Appendix.

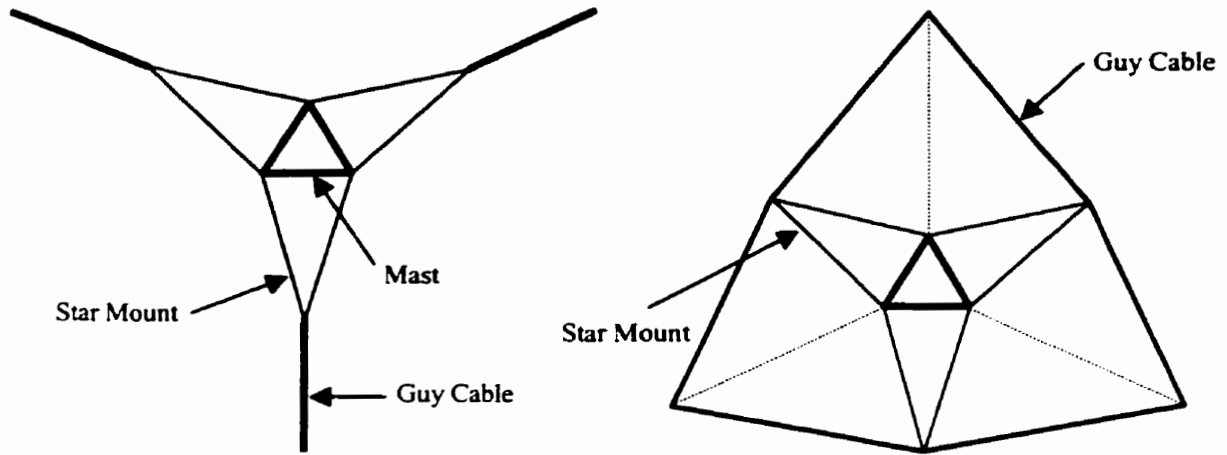


Figure 2.9: Guy configuration for tower with torsion arms (top view).

MICROWAVE SATELITE DISHES

A microwave dish is a small conical dish attached to the mast of a guyed tower via a short rigid link as shown in Figure 2.10. It does not provide any structural stiffness to a guyed tower. A satellite dish is incorporated into the structural model by considering it as a lumped mass.

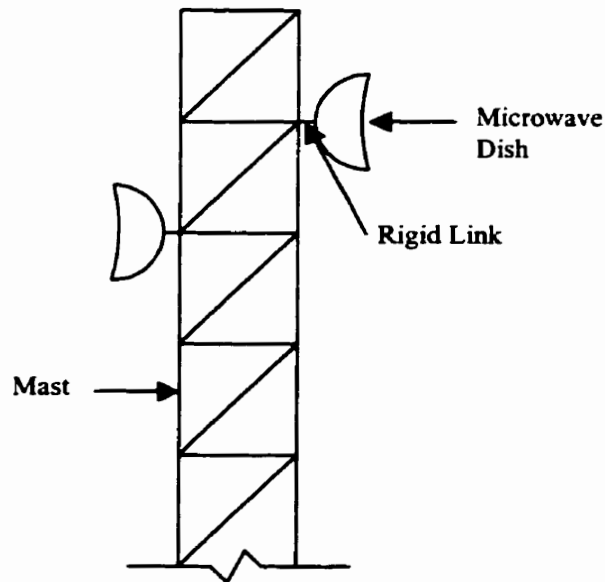


Figure 2.10: Microwave satellite dishes.

2.5 FREE VIBRATION ANALYSIS

When a displacement is applied to a structural system in a state of static equilibrium and then released, it freely vibrates about the static equilibrium position. Such vibrations are dependent upon the mass and stiffness of structure. The purpose of a free vibration analysis is to determine the natural frequencies and corresponding deflections referred to as modeshapes.

The natural frequencies and modeshapes of a structure obtained from a free vibration analysis can be very useful. The frequencies are an immediate indication of the resonance frequency of the structural system. Knowledge of such frequencies is useful in designing tower structures for gusty winds and other types of dynamic loading.

A simple spring-mass-dashpot model can be used to represent basic free vibration analysis of a structure. Consider the one-degree of freedom system shown in Figure 2.11. The dynamic equilibrium is expressed by

$$m\ddot{x} + c\dot{x} + kx = f(t) \quad (2.24)$$

where overdot indicates differentiation with respect to time. The equation of motion for an elastic system with a finite number of DOF may be expressed in matrix notation as

$$M\ddot{x} + C\dot{x} + Kx = F(t) \quad (2.25)$$

where M , C and K are the global mass, damping and stiffness matrices respectively, x is the vector of displacements for each DOF and $F(t)$ is a time-dependant load vector corresponding to each DOF.

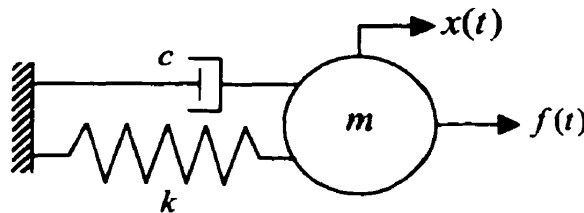


Figure 2.11: Dynamic equilibrium of a spring-mass-dashpot system.

In the case of a completely unconstrained ($F(t) = 0$) and undamped ($C = [0]$) structure undergoing free oscillations, the equation of motion (2.25) is reduced to

$$M\ddot{x} + Kx = 0. \quad (2.26)$$

The general solution of (2.26) can be expressed as

$$x(t) = \phi e^{i\omega t} \quad (2.27)$$

where ϕ is a vector of displacement amplitudes and ω denote frequency of motion.

Substitution of equation (2.27) into (2.26) gives

$$K\phi = \omega^2 M\phi. \quad (2.28)$$

This is an eigenvalue or characteristic value problem. From linear algebra, this equation has a non-trivial solution only if

$$|K - M\omega^2|\phi = 0. \quad (2.29)$$

Evaluating the determinant of equation (2.29) leads to a polynomial of order n (where n is the number of unconstrained DOF in the system). The roots of this polynomial give the free vibration (natural) frequencies, ω_i^2 , $i = 1 \dots n$. Back substitution of these frequencies into equation (2.28) results in n mode shape vectors, $\phi^{(i)}$.

The non-trivial solution of equation (2.29) is commonly obtained from a computer-based analysis. A common algorithm used to solve characteristic value problems is the Jacobi method. However, when the order of the stiffness and mass matrices is large, use of the Jacobi solution procedure can be very inefficient (Bathe 1982). Since a finite element analysis of a guyed tower system requires a solution to a large eigenvalue problem, the Jacobi method was not used in this study. Instead, the IMSL library subroutine GVCSP was utilized. The IMSL subroutine computes all of the eigenvalues and eigenvectors of the generalized real symmetric eigenvalue problem $Az = \lambda Bz$, with B symmetric positive definite. The Cholesky factorization $B = RTR$, with R a triangular matrix, is used to transform the equation $Az = \lambda Bz$, to $(R^{-T}AR^{-1})(Rz) = \lambda(Rz)$. The eigenvalues and eigenvectors of $C = R^{-T}AR^{-1}$ are then computed. The generalized eigenvectors of A are given by $z = R^{-1}x$, where x is an eigenvector of C . This development is found in Martin and Wilkinson (1968). The Cholesky factorization is computed based on IMSL routine LFTDS. The eigenvalues and eigenvectors of C are computed based on routine EVCSF.

Chapter 3

NATURAL FREQUENCIES OF CABLES AND BEAMS

3.1 COMPARISON OF CABLE FREQUENCIES

TIGHTLY STRETCHED CABLE

Certain verifications must be made to ensure the accuracy of structural model developed in the present study. An obvious case to consider initially is comparison of results obtained from the cable finite element developed in this study with the classical case of a tightly stretched cable (a horizontal cable with sufficient tension to overcome self-weight of the cable). For this special case, the in-plane and ‘sway’ (out-of-plane) modes obtained from the finite element analysis are shown to have identical natural frequencies that converged to the following classical result (Henghold et. al. 1977)

$$\Omega_n = n\pi\sqrt{T}; \quad n = 1, 2, 3, \dots \quad (3.1)$$

where $T = t/mgL_c$, and m and t represent the mass per unit length and cable tension respectively.

In addition, the non-dimensional frequency Ω in (3.1) is defined as

$$\Omega = \omega / \sqrt{\frac{g}{L_c}} \quad (3.2)$$

where ω is natural frequency of a cable in rad/sec, g is the acceleration due to gravity, and L_c is the chord length of the cable.

In addition to the identical in-plane and 'sway' modes, a bar mode was also identified in the analysis. This bar mode was shown to have natural frequencies that converged to the analytical result

$$\Omega_n = n\pi \sqrt{\frac{A_c E_c}{mgL_c}}. \quad (3.3)$$

HORIZONTAL CABLE

In the case of a horizontal sagging cable (Figure 3.1), a set of natural frequencies that include in-plane symmetric, in-plane anti-symmetric and out-of-plane modes were identified. The analytical solutions for the natural frequencies of a horizontal sagging cable were given by Irvine (1981).

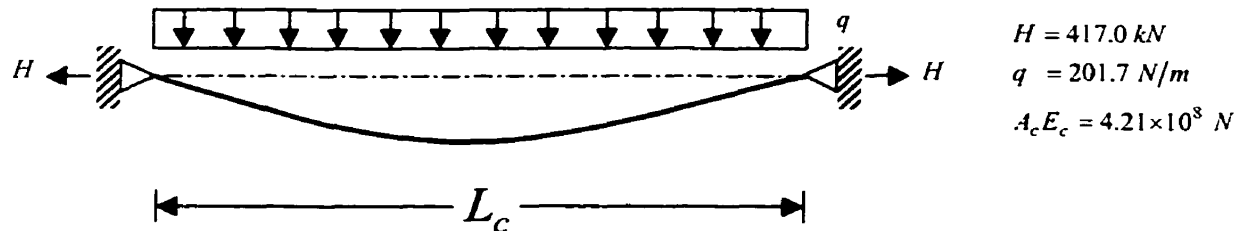


Figure 3.1: Horizontal sagging cable.

The Tables 3.1, 3.2 and 3.3 present a comparison of natural frequencies for in-plane symmetric, in-plane anti-symmetric and out-of-plane modes of the cable shown in Figure 3.1. For each mode, the first four transverse natural frequencies are presented for a cable discretized into eight and sixteen finite elements. Both lumped and consistent-mass idealizations were used in the comparisons. The results presented by Mathur (1985) correspond to a cable following a parabolic profile. As can be seen from the tables, eight cable elements produced reasonably accurate results (less than 10% error) for the first two natural frequencies. However, in the case of the third and fourth frequencies, the error was shown to range from 10-30%. In contrast, the use of sixteen elements produced results, which showed errors less than 8% for the first four natural frequencies. From the

results obtained, it was evident that a greater number of elements is required to obtain accurate solutions for the higher modes. The guyed tower analysis program developed in this study provides a user with an option to specify the number of finite elements to be used in the cable discretization.

Both lumped-mass and consistent-mass solutions were shown to converge to the analytical solution at a similar rate. For higher frequencies, the consistent-mass results were found to converge only slightly faster than lumped-mass based results except in the case of in-plane symmetric mode where the convergence rates were very similar. Based on this finding it appeared advantageous to implement the lumped-mass formulation in the software development to ensure computational efficiency. However, another interesting behavior was also observed. From the cases considered in Tables 3.1, 3.2 and 3.3, it appeared that the two different mass models converged to the analytical solution presented by Irvine (1981) from different directions. The consistent-mass formulation overestimated the analytical solution, while the lumped-mass formulation consistently underestimated the solution. A comprehensive literature search did not find any discussion on the two different mass models converging via different bounds, however a discussion on the rate of convergence for the two models was found. In a study by Tong et al. (1971), it was shown that the lumped-mass idealization suffers no loss in the rate of convergence for systems with low DOF (i.e. a rod). However, for problems governed by higher order equations (beam or plate), the consistent-mass approach was shown to yield better convergence. Since the guy cable model in this study comprises of three DOFs, the consistent-mass formulation provides better accuracy at a somewhat lower computational efficiency. As such, the software developed in this study provides a user with the option of choosing between the two different mass models.

λ^2	Length [m]	Normalized natural frequency (ω/π)					
		Mode	Lumped (8 elements)	Consistent (8 elements)	Lumped (16 elements)	Consistent (16 elements)	Irvine (1981)
60	506.3	1	2.27	2.33	2.29	2.30	2.29
		2	3.00	3.33	3.13	3.21	3.18
		3	4.24	5.77	4.81	5.22	5.03
		4	4.99	8.33	6.45	7.55	7.01
20	291.6	1	1.60	1.62	1.61	1.61	1.61
		2	2.86	3.20	2.99	3.08	3.04
		3	4.24	5.77	4.80	5.20	5.01
		4	4.99	8.34	6.46	7.55	7.00
6	159.6	1	1.21	1.23	1.22	1.22	1.22
		2	2.84	3.18	2.96	3.05	3.01
		3	4.23	5.76	4.80	5.20	5.00
		4	4.99	8.34	6.46	7.55	7.00
2	92.1	1	1.07	1.08	1.08	1.08	1.08
		2	2.83	3.18	2.96	3.04	3.01
		3	4.23	5.77	4.80	5.20	5.00
		4	4.99	8.34	6.46	7.55	7.00

Table 3.1: In-plane symmetric modes for a horizontal sagging cable.

λ^2	Length [m]	Normalized natural frequency (ω/π)					
		Mode	Lumped (8 elements)	Consistent (8 elements)	Lumped (16 elements)	Consistent (16 elements)	Irvine (1981)
60	506.3	1	1.94	2.04	1.98	2.00	2.00
		2	3.59	4.40	3.89	4.09	4.00
		3	4.70	7.15	5.65	6.34	6.00
		4	-	-	7.19	8.80	8.00
20	291.6	1	1.94	2.05	1.98	2.01	2.00
		2	3.60	4.41	3.89	4.10	4.00
		3	4.70	7.16	5.65	6.34	6.00
		4	-	-	7.20	8.81	8.00
6	159.6	1	1.95	2.05	1.99	2.01	2.00
		2	3.60	4.41	3.90	4.10	4.00
		3	4.70	7.16	5.66	6.35	6.00
		4	-	-	7.20	8.82	8.00
2	92.1	1	1.95	2.05	1.99	2.01	2.00
		2	3.60	4.41	3.90	4.10	4.00
		3	4.70	7.16	5.66	6.35	6.00
		4	-	-	7.20	8.82	8.00

Table 3.2: In-plane anti-symmetric modes for a horizontal sagging cable.

where $\lambda^2 = \frac{(mgl/H)^2 l}{HL_c/E_c A_c}$.

λ^2	Length [m]	Normalized natural frequency (ω/π)					
		Mode	Lumped (8 elements)	Consistent (8 elements)	Lumped (16 elements)	Consistent (16 elements)	Irvine (1981)
60	506.3	1	0.99	1.00	1.00	1.00	1.00
		2	1.95	2.05	1.98	2.01	2.00
		3	2.83	3.17	2.95	3.03	3.00
		4	3.60	4.40	3.89	4.10	4.00
20	291.6	1	0.99	1.00	1.00	1.00	1.00
		2	1.95	2.05	1.99	2.01	2.00
		3	2.83	3.17	2.95	3.04	3.00
		4	3.60	4.41	3.90	4.10	4.00
6	159.6	1	0.99	1.01	1.00	1.00	1.00
		2	1.95	2.05	1.99	2.01	2.00
		3	2.83	3.17	2.95	3.04	3.00
		4	3.60	4.41	3.90	4.10	4.00
2	92.1	1	0.99	1.01	1.00	1.00	1.00
		2	1.95	2.05	1.99	2.01	2.00
		3	2.83	3.17	2.96	3.04	3.00
		4	3.60	4.41	3.90	4.10	4.00

Table 3.3: Out-of-plane modes for a horizontal sagging cable.

INCLINED CABLE

In order to validate the cable finite element model for an inclined sagging cable, Table 3.4 compares the results obtained from the present study with those presented by Henghold et al. (1977). The configuration of cable used in the analysis is depicted in Figure 2.3, where θ is the angle of inclination of the chord line. The non-dimensional sag is defined as, $D = s/L_c$ where s is the maximum vertical displacement of the cable equilibrium position from the chord line to the length of the cable. Likewise, the chord length is also non-dimensionalized such that, $C = L_c/L_e$. Eight cable elements of equal length were used to model the cable. As can be seen from the results in Table 3.4, the present solution compares favorably with the solutions of Henghold et al. (1977). A more complete comparison for a greater range of non-dimensional sag D to the natural frequencies was made by reproducing Figures 2 and 3 from Henghold et al. (1977). The non-dimensional frequency Ω was plotted against the non-dimensional sag D in Figures 3.4, 3.5 and 3.6. It can be seen that these figures are almost identical to the Figures 2 and 3 of Henghold et al. (1977). Furthermore, in a paper by Irvine (1978), analytical equations for free vibrations of an inclined cable were presented. These equations may be used to re-produce much of the data depicted in Figures 2 and 3 from Henghold et al.

(1977). The cable element used in this study is much simpler and it compares favorably with the fully non-linear solutions presented by Henghold et al. (1977). Therefore, it can be concluded that present 2-node cable element is capable of accurately representing the behaviour of inclined cables attached to a tower mast.

	$\theta = 0^\circ, D = 0.137$		$\theta = 30^\circ, D = 0.155$		$\theta = 60^\circ, D = 0.251$	
	Henghold	Present	Henghold	Present	Henghold	Present
Ω_1	3.02	3.00	2.83	2.83	2.24	2.25
Ω_2	5.65	5.61	5.17	5.19	3.65	3.61
Ω_3	6.05	6.04	5.67	5.72	4.53	4.58
Ω_4	8.77	8.81	8.17	8.26	6.30	6.32

Table 3.4: Chord inclination effects ($AE/mgL_c = 5000, C = 0.95$).

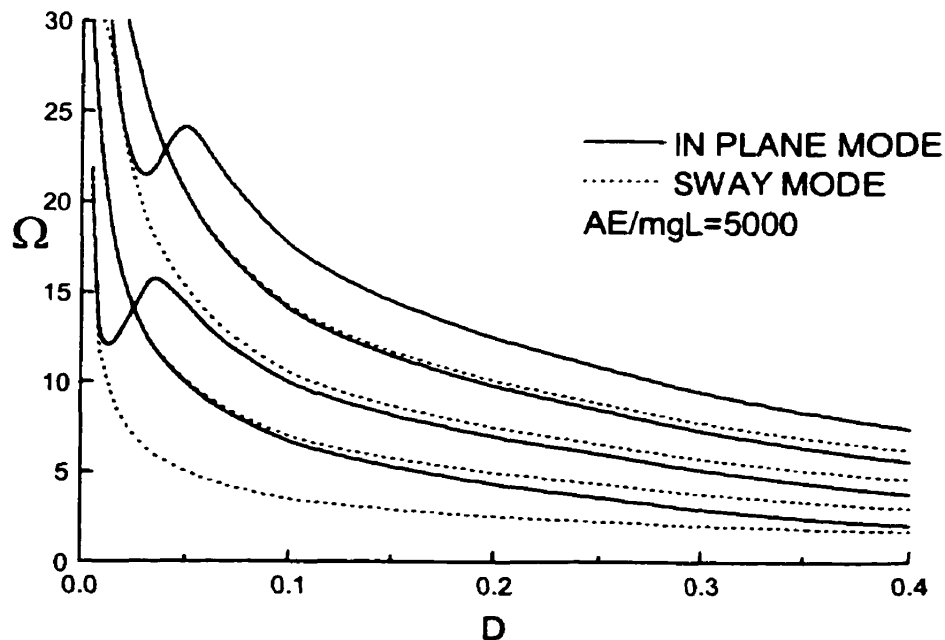


Figure 3.2: Variation of natural frequency with sag ratio for a horizontal cable.

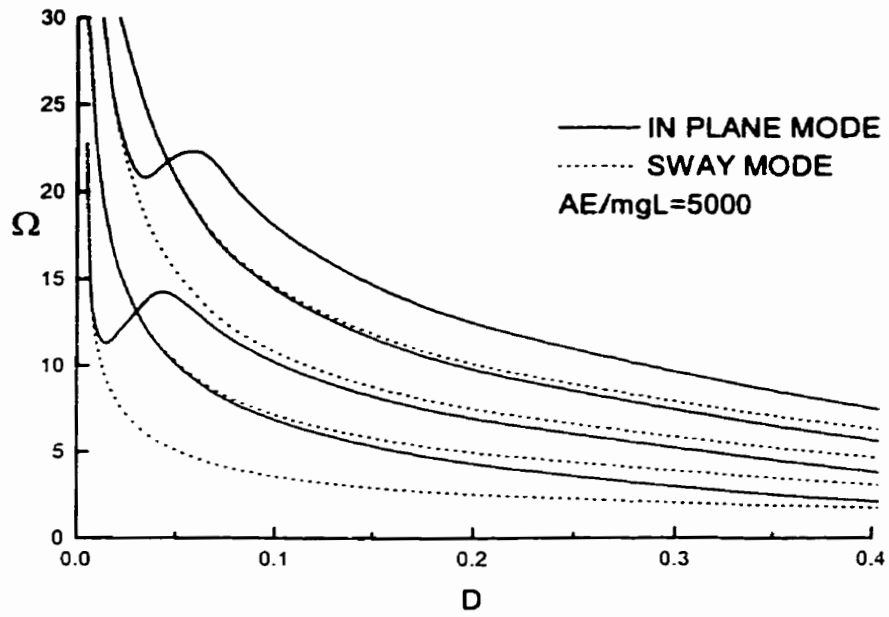


Figure 3.3: Variation of natural frequency with sag ratio for a cable inclined at 30° .

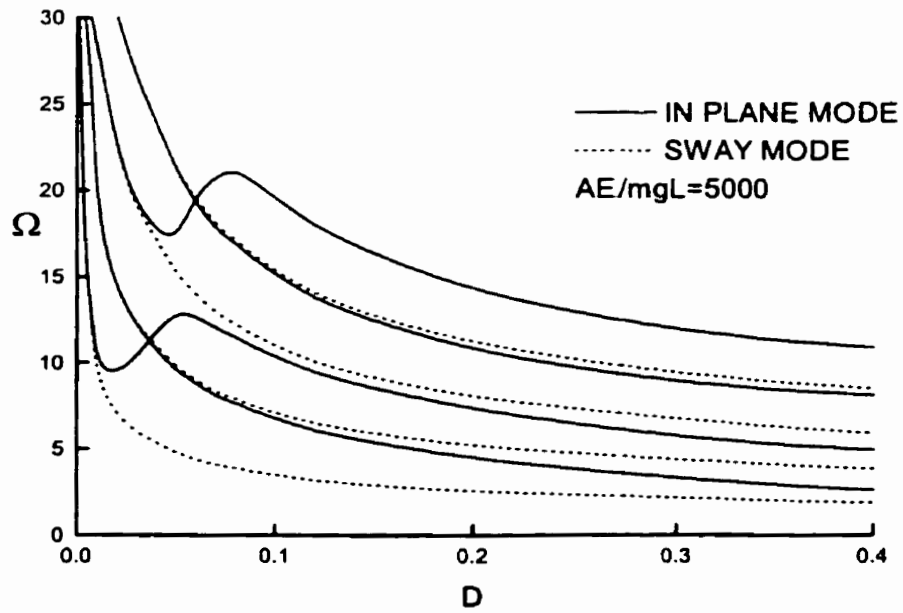


Figure 3.4: Variation of natural frequency with sag ratio for a cable inclined at 60° .

A comparison of the equivalent elasticity approach for an inclined cable with the catenary based finite element solutions was made to examine the accuracy of equivalent elasticity approach. In the equivalent elastic modulus approach, the cable was oriented along the chord length. An analysis of a tightly stretched cable showed convergence to the analytical solution of a tightly stretched cable (equations 3.2 and 3.3). However, the sag of a cable is not explicitly considered in the equivalent elasticity approach. Since the sag of the cable is neglected, the in-plane and out-of-plane frequencies are identical. Hence, it can be expected that the analysis provides reasonable results for the out-of-plane frequencies, but not for the in-plane frequencies. Table 3.5 shows a comparison of the catenary based finite element solution with the equivalent elasticity based finite element solution. Eight cable elements of equal length were used to model the cable.

D	0.050		0.075		0.125	
	Catenary	Equivalent	Catenary	Equivalent	Catenary	Equivalent
Ω_1	4.99	4.67	4.05	3.78	3.12	2.91
Ω_2	10.06	4.67	8.05	3.78	5.13	2.93
Ω_3	10.18	9.51	8.25	7.71	6.31	5.93
Ω_4	14.61	9.51	12.06	7.71	9.18	5.93

Table 3.5: Comparison of catenary and elasticity solutions ($\theta = 30^\circ$, $AE/mgL_c = 5000$).

As expected, Table 3.5 shows that the equivalent elasticity approach provides reasonable results for the out-of-plane frequencies (Ω_1 and Ω_3), but not for the in-plane frequencies (Ω_2 and Ω_4). As such, the equivalent elasticity approach was not implemented in this study.

3.2 COMPARISON OF BEAM FREQUENCIES

To verify the accuracy of beam finite element model used for tower mast, comparisons were made with the analytical torsional, flexural and axial vibration modes

for an elastic cantilevered beam. In addition to comparing the natural frequencies, the various mode shapes obtained were also examined against analytical results. The comparisons were done by considering a circular cantilever beam, with the following material properties.

Length of the beam: $L = 8 \text{ m}$.

Modulus of elasticity: $E = 200000 \text{ MPa}$.

Radius: $r = 0.075 \text{ m}$.

Density: $\rho = 8 \times 10^3 \text{ kg/m}^3$.

TORSIONAL VIBRATIONS

The analytical solution for natural frequencies corresponding to torsional vibration modes of a circular cantilever beam is given by (Inman 1996)

$$\omega_n = \frac{2(n-1)\pi c}{2L}, \quad n = 1, 2, 3, \dots \quad (3.4)$$

where $c = \sqrt{\frac{G\gamma}{\rho J}}$, (3.5)

G is the shear modulus, J is the polar moment of inertia and γ is a torsion constant shown and a circular cross section

$$\gamma = \frac{\pi r^4}{2}. \quad (3.6)$$

Natural Frequency	ω_{11}	ω_{12}	ω_{13}	ω_{14}
Analytical Solution	0.609	1.827	3.044	4.262
1 Element	0.671	-	-	-
4 Elements	0.613	1.933	3.511	5.078
8 Elements	0.610	1.853	3.167	4.599
16 Elements	0.609	1.833	3.075	4.346

Table 3.6: Comparison of torsional vibration frequencies.

FLEXURAL VIBRATIONS

The analytical solution for natural frequencies corresponding to flexural modes of a circular cantilever beam are given by (Chopra 1995)

$$\omega_{fn} = (\beta_n L)^2 \sqrt{\frac{EI}{mL^4}}, \quad n = 1, 2, 3, \dots \quad (3.7)$$

where

$$\beta_n L = 1.875, 4.694, 7.854, 10.998. \quad (3.8)$$

Natural Frequency	ω_{f1}	ω_{f2}	ω_{f3}	ω_{f4}
Analytical Solution	10.30	64.55	180.77	354.21
1 Element	10.35	-	-	-
4 Elements	10.30	64.63	182.16	359.36
8 Elements	10.30	64.56	180.87	355.01
16 Elements	10.30	64.56	180.77	354.27

Table 3.7: Comparison of flexural vibration frequencies.

AXIAL VIBRATIONS

Natural frequencies associated with axial vibration modes are very high and generally do not affect the dynamic response of guyed towers. The analytical solution for the natural frequencies corresponding to axial vibration modes of a circular cantilever beam is given by (Clough and Penzien 1975)

$$\omega_{an} = \frac{2n-1}{2} \pi \sqrt{\frac{EA}{mL^2}}, \quad n = 1, 2, 3, \dots \quad (3.9)$$

Natural Frequency	ω_{a1}	ω_{a2}	ω_{a3}	ω_{a4}
Exact Solution	981.75	2945.24	4908.74	6872.23
1 Element	1082.53	-	-	-
4 Elements	988.07	3116.99	5662.13	8187.93
8 Elements	983.32	2987.99	5107.44	7416.40
16 Elements	982.14	2955.90	4958.16	7008.14

Table 3.8: Comparison of axial vibration frequencies.

From the observed natural frequencies for a circular cantilevered beam (Tables 3.6 to 3.8), it was shown that for higher modes, additional elements were required in the analysis to obtain reasonably accurate results. This is similar to the case of a cable element. The use of eight elements yielded results within 8% of the analytical solutions, while the use of sixteen elements resulted in a maximum discrepancy of 2% for the first four modes. It was further identified from the results that the natural frequencies in torsional motion occur at much lower frequencies in comparison to flexural and axial motion. In fact, it would not be expected under normal circumstances that axial frequencies of a tower would be a concern given the higher frequency values involved. Furthermore, it is expected that the use of multiple guys and star mounts (torsion arms) would increase the overall stiffness of a tower mast and thereby increases the natural frequencies.

3.3 EQUIVALENT BEAM-COLUMN REPRESENTATION

Prismatic elements can be readily modelled as beam elements, which resist bending, torsional and axial loads and represented by stiffness and mass matrices. However, the development of mass and stiffness for a lattice structure is not as straightforward. One approach is to model a lattice structure as a space frame using a computer software package such as SAP90™. This approach can be very tedious and will require a significant computational effort. A simple and efficient way to analyze a

lattice tower is possible through the adoption of an approximate method of analysis. As previously mentioned, the latticed tower mast may be represented by an equivalent beam-column. As shown in Chapter 2, Kahla (1993) presented equivalent beam-column properties for latticed tower masts of triangular and square cross-section. The equivalent properties presented by Kahla (1993) were adopted in the present study. However, Mathur (1985) and Saxena (1988) utilized a similar approach to represent a latticed tower mast. Mathur (1985) presented stiffness and consistent mass matrices based on an assumed modeshape. It was shown that the solution for the equilibrium position of a tapered beam was a logarithmic function and that a cubic polynomial was the exact solution for a straight beam.

For a typical tapered or straight lattice segment with a square cross-section and supported by four continuous legs as shown in Figure 3.5, Mathur (1985) presented an equivalent beam-column representation.

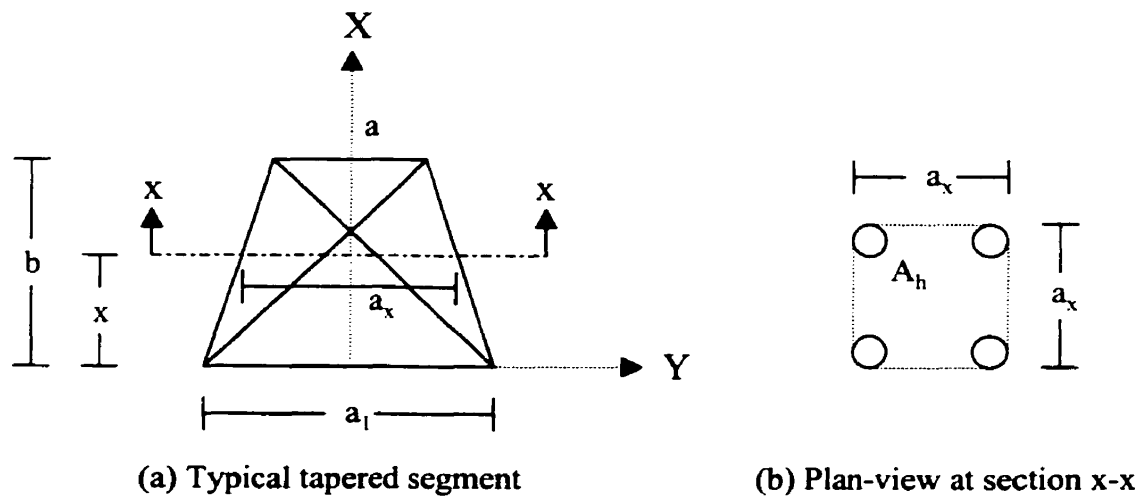


Figure 3.5: Latticed tower segment

The moment of inertia, $I(x)$, about the segments longitudinal axis x , at section x-x was given by

$$I(x) = A_h a_x^2 \quad (3.10)$$

where $a_x = a_1(1 - \beta x)$

and $\beta = \frac{a_1 - a}{a_1}$.

Hence, for a straight latticed tower segment, $a = a_1 = a_x$, therefore $\beta = 0$ and $I(x) = A_h a^2$. Similarly, Kahla (1993) shown that the equivalent flexural stiffness (EI) for a latticed mast with square cross-section is

$$EI = EA_h a^2 \quad (3.11)$$

for tower lacing patterns 1 to 4 and

$$EI = Ea^2 \left(A_h + \frac{A_s A_d \cos^3 \theta}{2(A_s + 2A_d \sin^3 \theta)} \right) \quad (3.12)$$

for lacing pattern 5. As can be seen from the above equations, the flexural stiffness presented by Mathur (1985) is identical to that presented by Kahla (1993) for lacing patterns 1 to 4. However, it can be seen that a slight variation in flexural stiffness exists between the two approximations for pattern 5. To compare the two approximate methods, consider the latticed tower shown in Figure 3.6

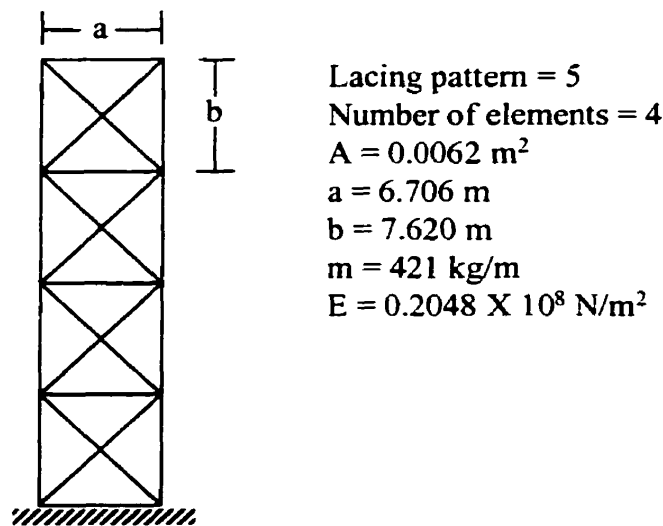


Figure 3.6: Latticed tower mast.

Table 3.9 shows the results of a free vibration analysis for the tower mast shown above in Figure 3.6. The table compares the analytical results with those obtained by Mathur (1985) and the present study. As can be seen from the results, the present study gives results that are consistent with the analytical solution and Mathur (1985).

	Natural Frequency (rad/sec)		
Mode	Analytical Results	Mathur (1985)	Present Study
1	0.440	0.440	0.440
2	2.757	2.760	2.760
3	7.715	7.779	7.774
4	15.085	15.340	15.304

Table 3.9: Comparison of flexural vibration frequencies.

Chapter 4

SOFTWARE DEVELOPMENT

Software developed in this study consists of an interactive Windows™ 95/98/2000 program for the free vibration analysis of a guyed tower. This chapter discusses the development of software package and provides use instructions. The software consists of two main components, a graphical user interface (GUI) and a finite element engine (FEE). The two components are discussed in detail with the aid of flow charts describing the software structure, interaction and algorithm.

4.1 GRAPHICAL USER INTERFACE (GUI)

The GUI acts as the front and back end to the finite element engine (FEE), respectively referred to as the pre and post-processors. The flow chart shown as Figure 4.1 describes the interaction between pre and post-processor (GUI) and the FEE. The GUI of the software package was developed utilizing the programming language Microsoft® Visual Basic®, which is an object-oriented programming language. An object-oriented programming language is similar to traditional programming languages in the sense that they both utilize a similar programming syntax, but has the further capability to facilitate the detailed development of graphical and menu driven software.

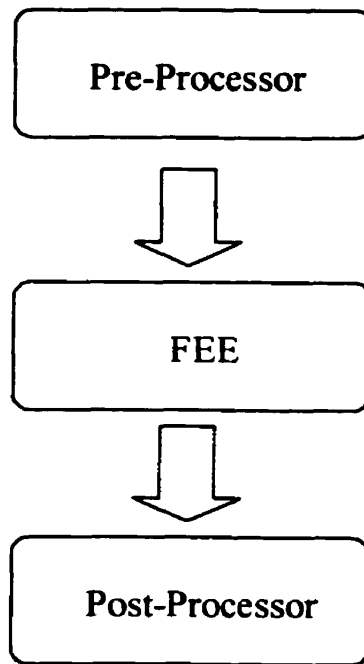


Figure 4.1: General program interaction.

However, unlike a traditional sequential programming language, object-oriented programming languages do not execute code at the beginning and sequentially work through the code line by line. Conversely, object-oriented programs are event driven. In this regard, programming code is assigned to different objects embedded within the interactive graphical program and the associated code does not execute until the specific event occurs for the object. In the Microsoft® Windows™ environment, an object traditionally consists of any item that exists in a Windows™ application. A command button, text box and menu bar are just a few examples of many possible objects. Furthermore, an event is an action that takes place on or within an object. Typical examples of an event are a single or double-click of the mouse on an object. Consider the following example, a command button (object) may have two different sets of code attached to it via two different events. In this example, code A and B are respectively assigned to the single and double-click event. Thus, when the user uses the mouse to click the command button (object) once, the single-click event has occurred and the software executes the associated code A. In a similar manner, if the command button had been double-clicked, code B would have been executed. In this regard, event driven

programming languages are driven by events occurring on or within objects. Thus, a user determines which segments of the code are executed based on the objects and events that are chosen.

4.2 PRE-PROCESSOR AND POST-PROCESSOR

In the past, the analysis of guyed towers has involved creating long and complicated data files that contain much of structural and modelling data. In an effort to move away from this tedious and often time consuming task, the interactive graphical pre-processor developed in this study collects all data required for a representative analysis and completes all of the data file preparation. Once the necessary data has been collected, the pre-processor creates the necessary data files to be used by the FEE for the analysis of a guyed tower. The pre-processor collects the data specific to the analysis from a user in a friendly and non-tedious interactive manner. As the necessary data is collected from a user, the pre-processor completes several checks in an effort to ensure that no inconsistencies exist in the data. Where inconsistencies are identified, a user is promptly alerted with a warning message outlining the nature of inconsistencies. The data files are then used by the FEE to complete the numerical analysis of the tower model.

Once the numerical analysis has been completed, a user has the option of utilizing the post-processor tools to view the results of the analysis. Similar to the pre-processor, the post-processor is an interactive graphical tool that may be used to view the results of the free vibration analysis in a graphical or non-graphical manner. Utilizing the data file created by the FEE which contains all the natural frequencies and modeshapes of the tower, the post processor provides the user with a variety of options to portray the data. These options include a file viewer that enables a user to view the natural frequencies and modeshapes of the analysis. In addition, the software has a graphical animation tool that provides a user with the option of viewing the animated modeshapes of the guyed tower system.

4.3 FINITE ELEMENT ENGINE (FEE)

The FEE created for this study was developed utilizing the Microsoft® Fortran Power Station Developer Studio. This powerful application allows the development of software utilizing Fortran programming language. The Developer Studio comes with a complete set of built-in IMSL math libraries that may be linked to the software being developed. The FEE consists of two main components, the model generator (*eqvbeam*) and numerical algorithm (*gtap*). A flow chart describing the layout and interaction between the two FEE components is shown in Figure 4.2. Utilizing the parameters collected by the pre-processor from a data file, the model generator computes a beam-column of equivalent stiffness utilizing the scheme outlined in Chapter 2 to represent the mast of a guyed tower. Once the equivalent beam-column has been determined, the model generator uses the model parameters previously collected to create a single data file that contains all the modelling data for a guyed tower.

At this point the numerical algorithm utilizes the model data to create a finite element model and subsequently conduct a free vibration analysis of the guyed tower model. The structural mass and stiffness matrices presented earlier in this study are used to numerically represent the tower mast and attached guy cables. Using the concept of destination vectors, the individual mass and stiffness matrices for each element are assembled into a global mass and stiffness matrix. Having assembled the global matrices, the final task of the FEE is to solve the generalized free vibration problem as previously discussed in Chapter 2. The eigenvalue problem is solved using the DGVCSP subroutine included with the built-in IMSL libraries. As the analysis is conducted, the natural frequencies and mode shapes are stored in a new data file which is later used by the post-processor to display mode shapes.

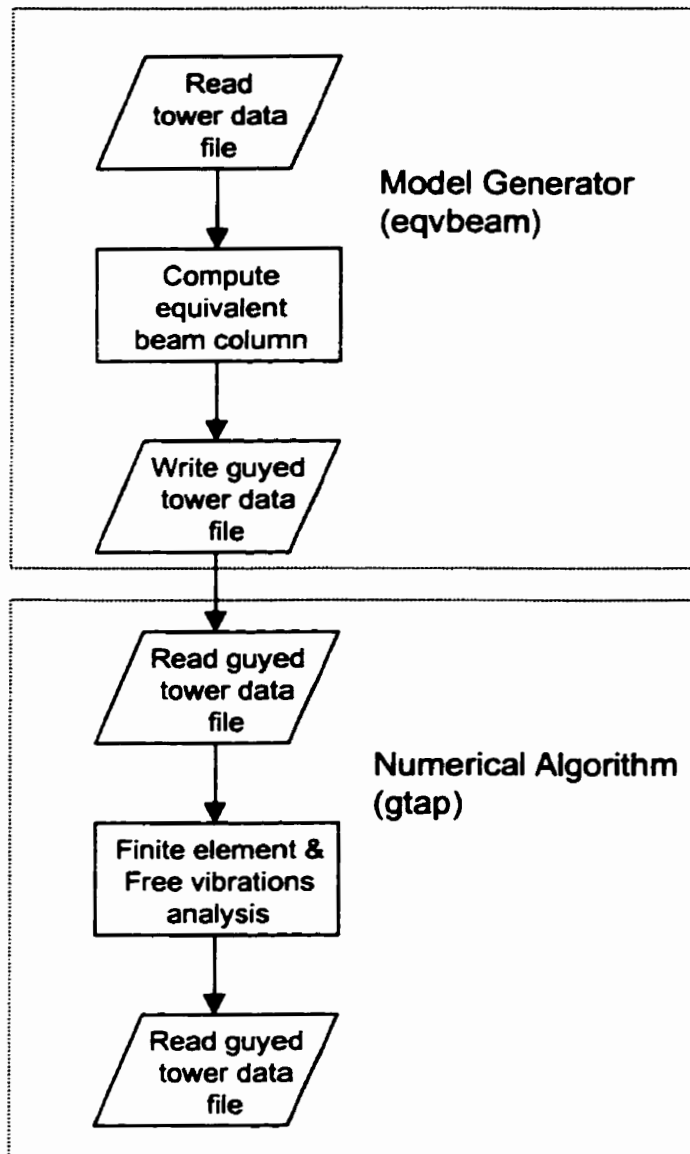


Figure 4.2: FEE program interaction.

4.4 SOFTWARE INSTALATION

INSTALATION REQUIREMENTS

In order to use the GTAP software, the following is a list of the minimum system requirements:

- A compatible PC equipped with the Windows™ 95/98/2000 operating system.

- 4 MB of free hard disk space.
- Windows™ compatible hardware.
- A 3½ inch floppy disk drive.
- IMSL software user license.

INSTALLING GTAP

1. Insert the *GTAP Installation Disk 1* into the floppy disk drive that will be used to install the software package.
2. Select the *Run...* icon from the Windows *Start* button.
3. If you are installing the software from *Drive A*, issue the following command; *a:setup* and click the *OK* button. If you are installing the software from a disk drive other than *Drive A*, substitute the command *a:setup* with the appropriate drive letter (for example, *b:setup*).
4. At this point, the *GTAP Installation Wizard* should begin and appear on the screen. The *Installation Wizard* provides you with detailed step by step instructions throughout the software installation process. It is strongly recommended that the GTAP software be installed in the default directory *c:\Program Files\GTAP*.

4.5 SOFTWARE INSTRUCTIONS AND MODEL DEVELOPMENT

1. Ensure that the GTAP software has been successfully installed onto the PC.
2. Select the *Programs* icon from the *Start* menu. A list of software programs should appear. From this list, select the *GTAP* icon. If you wish to make a shortcut to the GTAP program, or relocate the software on the *Start* menu, consult the online *Help* located in the program list on the *Start* menu.
3. Once the GTAP software completed loading, the initial welcome screen will appear. Once you have read the welcome screen, press the *Continue* button to carry forward. At this point, the main GTAP window as shown in Figure 4.3 should appear. From the main GTAP window and utilizing the options from the main menu, the user may access the various program features such as the *File* area, the *Define* options (pre-

processor), conduct a free vibration *Analysis*, view the analysis *Results* (post-processor) or consult the online *Help*.

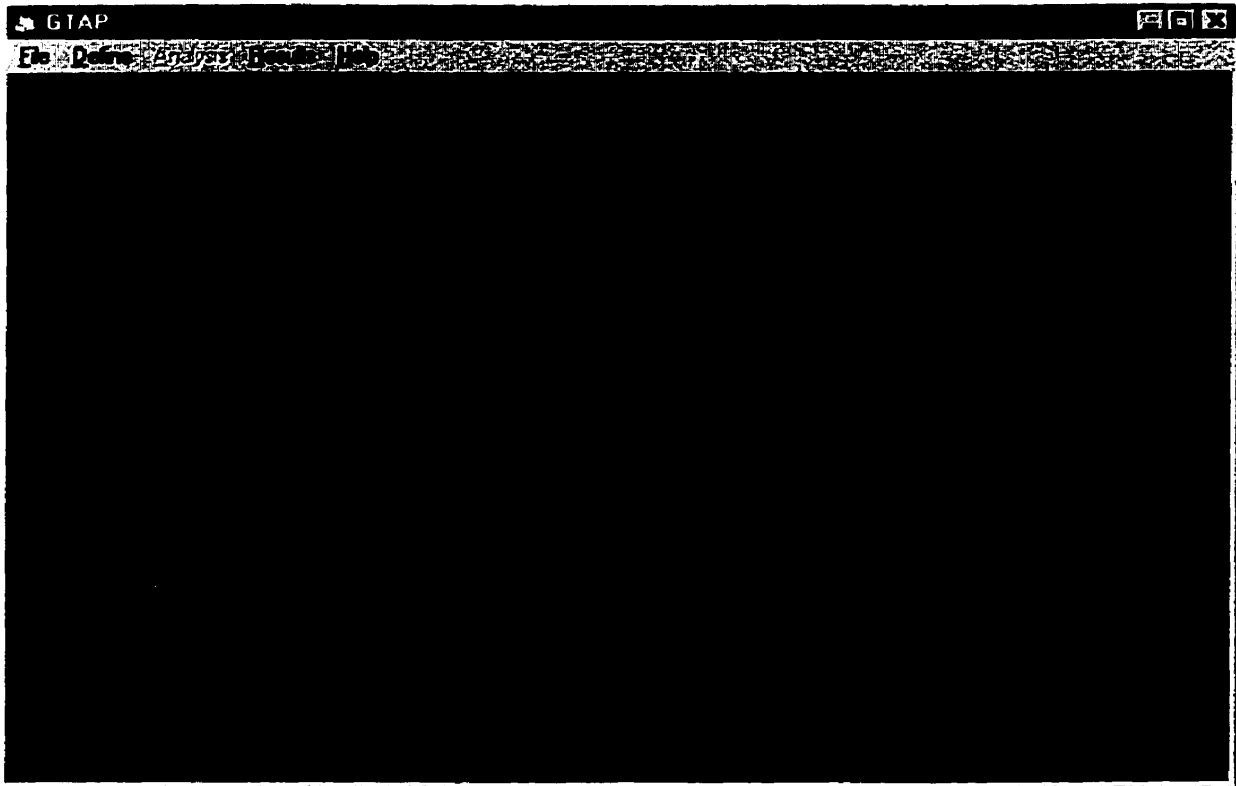


Figure 4.3: Main GTAP window.

The following steps outline how to create a representative guyed tower model utilizing the GTAP software.

1. From the *Define* menu located in the main GTAP window, select the item *Project*. The *Project Information* window as shown in Figure 4.4 should appear. Within this window, the user should enter the descriptive data that are used to identify the model. Once the three text boxes have been completed, select the *OK* button to carry forward.
2. Utilizing the mouse or keyboard, select the *Tower Base* item from the *Define* menu. The *Tower Base* window as shown in Figure 4.5 should now appear. From this window, the user shall specify the base restraint conditions to be used at the base of the guyed tower model. Utilizing the mouse or keyboard, select the radio button that

best represents the restraining conditions at the base of the guyed tower (pinned or fixed). Once the appropriate base condition has been selected, press the *OK* button to continue.

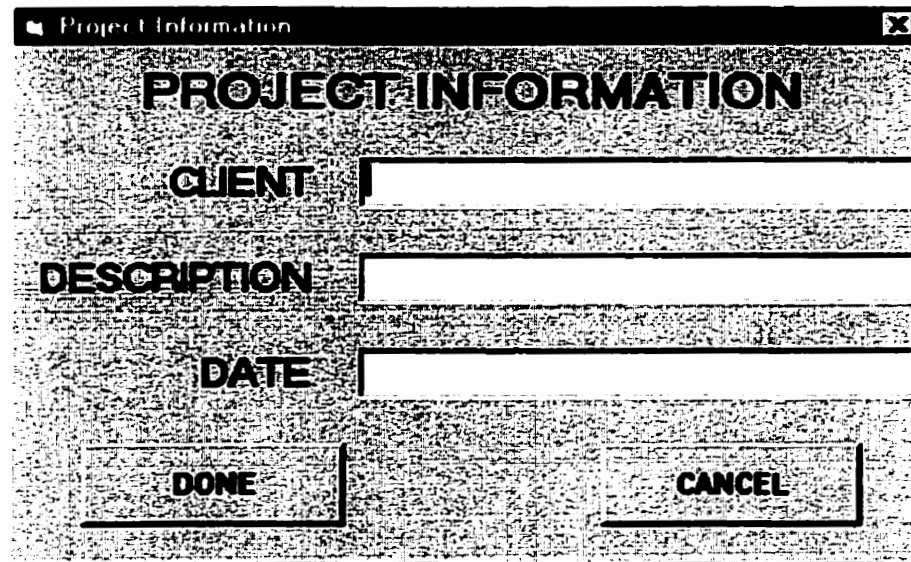


Figure 4.4: Project Information window.

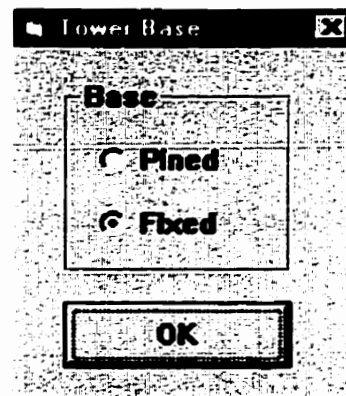
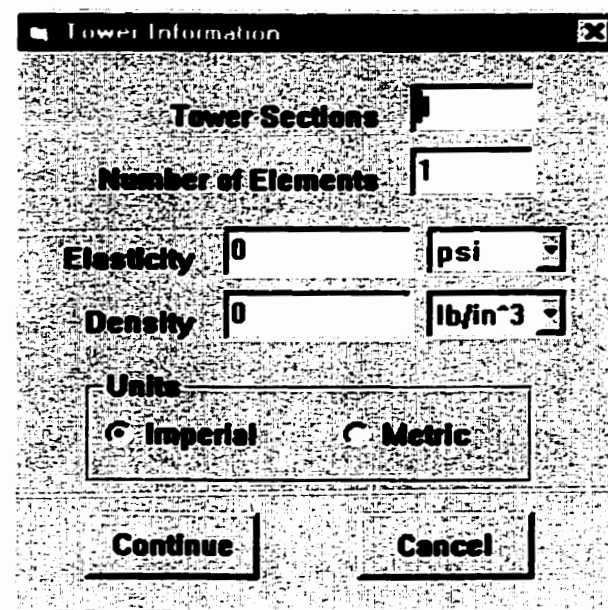


Figure 4.5: Tower Base window.

3. Following the steps above, select the *Tower Information* item from the *Define* menu. Once the item has been selected, the window as shown in Figure 4.6 should appear. From this window, the user shall define several of the guyed tower parameters pertaining to the mast. Prior to proceeding any further in the development of a guyed tower model, the user should have a good idea of the configuration of the model. The first text box that should be completed is *Tower Sections*. In this text box, a user

should enter the integer value which denotes how many different tower sections are to be included in the entire tower. Generally, each different lacing pattern requires its own tower section. Next the user should enter how many tower elements are to be included in the model. Once the above two text boxes have been completed, the user should enter representative material properties for the tower mast. The final information that is requested from this window is your preference of units to be used in the analysis. Once the window has been completed, select the *Continue* button to carry forward. Provided that no inconsistencies were identified with the entered data, the window disappears and the main GTAP window shall once again appear.



The image shows a dialog box titled "Tower Information" with a close button (X) in the top right corner. The dialog contains the following fields and controls:

- Tower Sections:** A text input field that is currently empty.
- Number of Elements:** A text input field containing the value "1".
- Elasticity:** A text input field containing "0" and a dropdown menu set to "psi".
- Density:** A text input field containing "0" and a dropdown menu set to "lb/in³".
- Units:** A section with two radio buttons: "Imperial" (which is selected) and "Metric".
- Buttons:** Two buttons at the bottom: "Continue" and "Cancel".

Figure 4.6: Tower Information window.

4. From the main menu select the item *Tower Sections* and a window as shown in Figure 4.7 should appear. For each different tower section, the user will be prompted to complete the form shown in Figure 4.7. Online help is available to show various lacing patterns and the locations of the lacing dimensions on a tower. Once the form has been completed use the *Next* and *Back* buttons to navigate through the various *Tower Section* forms. When the final form has been completed, the *Tower Sections* window will close.

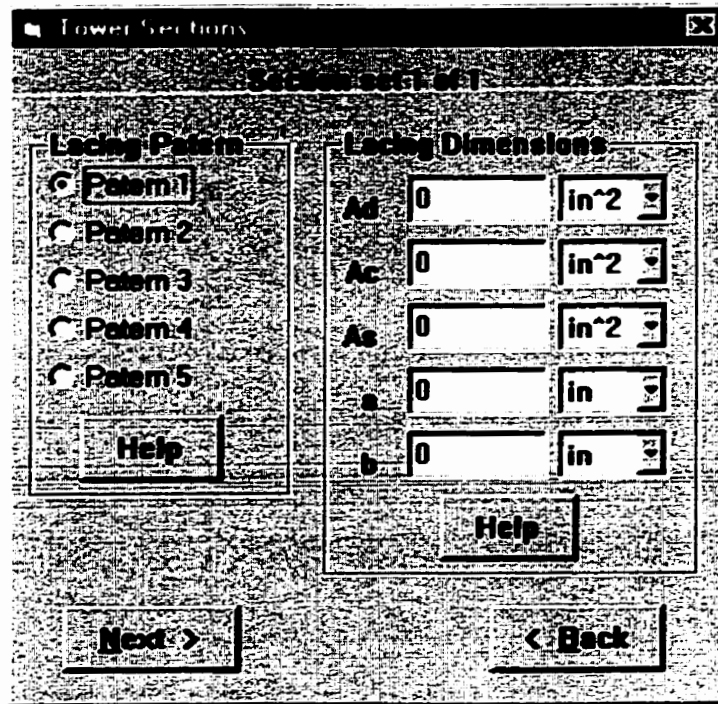


Figure 4.7: Tower Sections window.

5. The final steps involved in the development of a model for the mast of a guyed tower is to define the properties of the individual elements of the tower. From the *Elements* window shown in Figure 4.8, the user needs to specify the length and corresponding Tower Section for each tower element. Furthermore, the user also has the option of restraining the element by removing the check marks from the restraint boxes. Once the form has been completed the user may navigate through the forms for each element utilizing the *Next* and *Back* buttons until a form has been completed for each element.

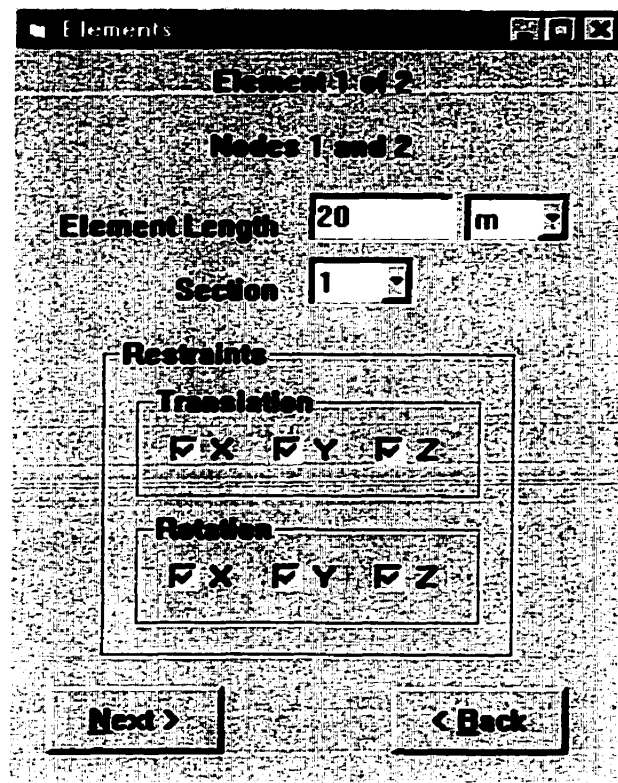


Figure 4.8: Elements window.

6. Next, the guy and torque arms data is entered. From the *Define* menu, choose the *Guy + Guy Rings* option. The *Guy Cables* window as shown in Figure 4.9 should now appear. In this window enter the number of guys, guy rings and the material properties of the guy cables. The concept of guy rings is discussed in the detailed example contained in Appendix B. Once all the fields in the *Guy Cables* window have been completed, press the *Continue* button. At this point the *Guy Cables* window closes and the *Guy Rings* windows as shown in Figure 4.10 appears. In this window, the user needs to enter the co-ordinates for each anchor location along the guy ring. Each guy ring contains three anchors as the software assumes that the cables are evenly spaced at 120° . Using the *Next* and *Back* buttons, the user may navigate through the various windows until all the co-ordinate locations have been accounted for.

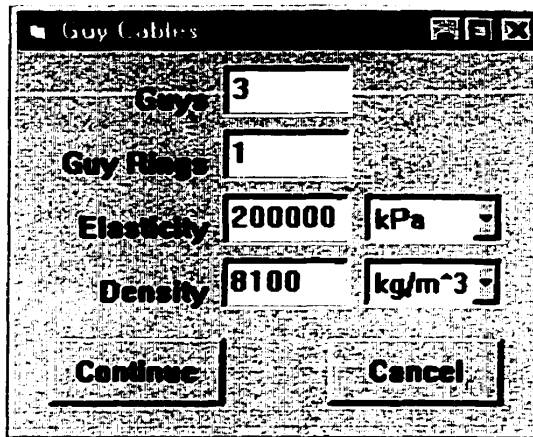


Figure 4.9: Guy + Guy Rings window.

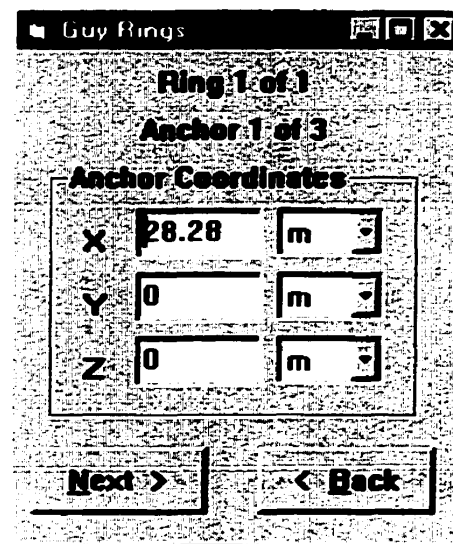


Figure 4.10: Guy Rings window.

7. The final step in development of the model is to complete the *Guy Cable* window accessible from the *Define* menu. Once that item has been selected, the *Guy Cable* window as shown in Figure 4.11 appears. Utilizing the drop down boxes, select which ring, anchor and node on the mast where the guy cable is connected. Furthermore, enter the area and pre-tension force of the guy cable. Use the *Next* and *Back* buttons to navigate through the various windows for all the cables.

Once the *Guy Cable* form is completed, the guyed tower model has been completed. As such, the pre-processor (*Define* menu) is no longer required. However, the user may recall any of the *Define* items to change any of the model parameters entered thus far.

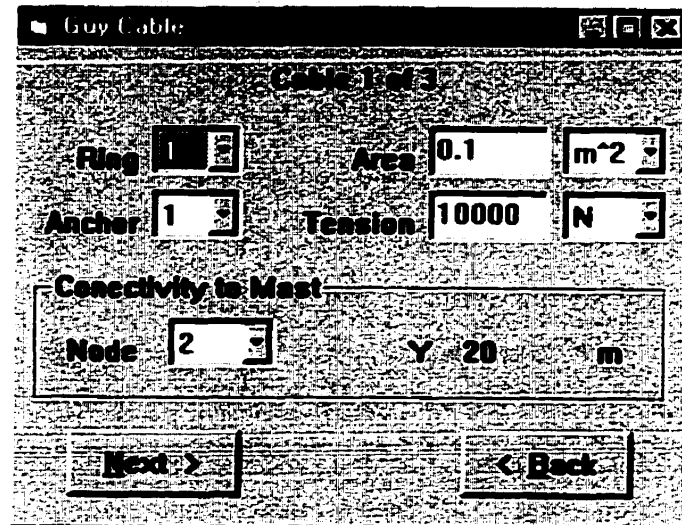


Figure 4.11: Guy Cable window.

Once all of the pre-processor items from the *Define* menu have been successfully completed, the *Analysis* menu will become available and free vibration analysis may be conducted for the guyed tower model. To begin the analysis, select *Begin* from the *Analysis* menu. This process may take up to a few minutes to complete depending on the size of the problem and processor speed of the computer.

During the analysis phase, the finite element engine generates a structural model of the guyed tower based on the data entered into the pre-processor. Once the analysis is complete, the results are stored in several data files and the *Results* menu (post-processor) now becomes available. By selecting the *Post-Processor* item from the *Results* menu the *Post-Processor* window as shown in Figure 4.12 will appear. From this window the user has the option of either viewing the natural *Frequencies* in text format from a data file or viewing the natural frequencies and associated *Modeshapes* of the guyed tower model. If the user chooses to view the animated modeshapes, an animation window as shown in Figure 4.13 will appear. Depending on the frequency chosen by the user, either an in-plane or out-of-plane view of the tower will be shown. Using various controls the user can begin and change the speed of the animation. By using the drop down box from the main *Post-Processor* window the user may view the modeshapes for any of the natural frequencies.

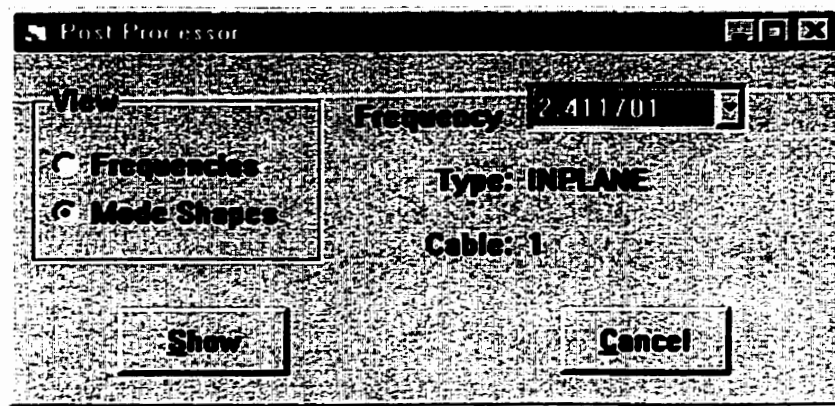


Figure 4.12: Post Processor window.

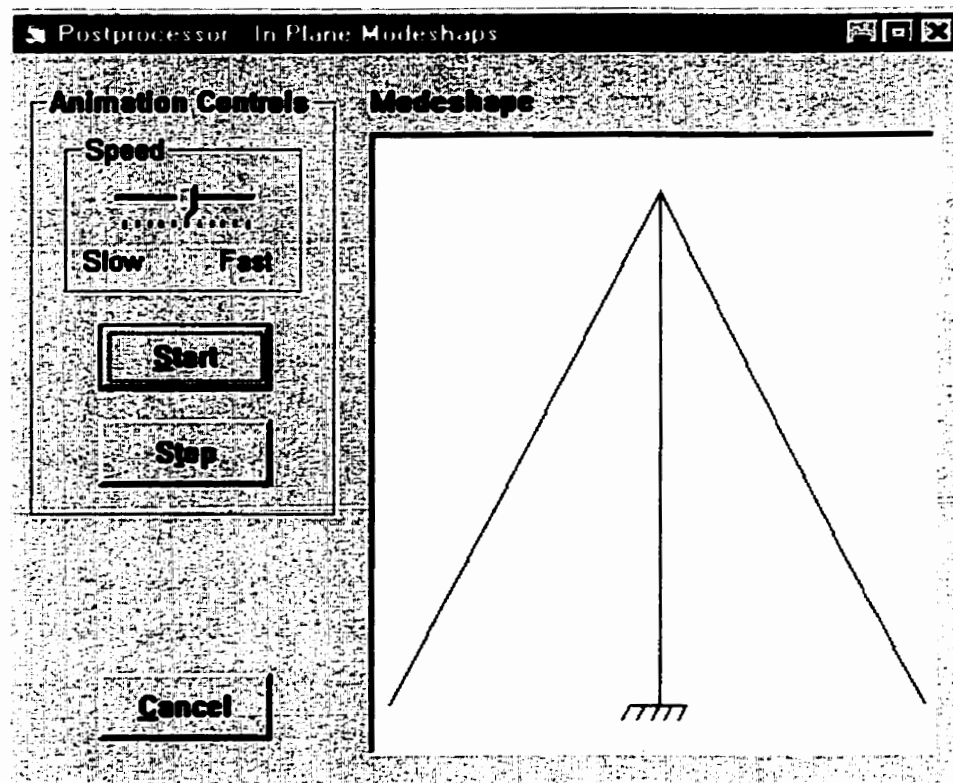


Figure 4.13: Post Processor – Animated Modeshapes.

Chapter 5

FREE VIBRATION CHARACTERISTICS OF GUYED TOWERS

5.1 WTMJ TOWER

The WTMJ tower is a 300 meter television tower located in Milwaukee, Wisconsin. This symmetric tower is supported by five levels of guys each having three guy cables equally spaced (120°) from one another. Each guy cable is attached directly to the mast of the tower. McCaffrey (1969) presented details of the tower geometric and structural properties. For completeness, the guyed tower properties have been included in the Appendix.

NATURAL FREQUENCIES

Prior to conducting free vibration analysis of the entire tower, a dynamic analysis of individual guy cables at each guy level was completed. This analysis was completed in an attempt to determine if and how the analysis of individual guy cables may be utilized in an effort to help predict the response of guy cables when attached to the mast of a tower. The guy cables were each modelled by sixteen cable elements. The free vibration results are presented for two different cable elements, the catenary cable

element presented in Chapter 2 and a parabolic cable element based on the analytical formulation presented by Veletsos and Darbe (1983).

Guy Level	Excited Mode	Frequency (rad/sec)	
		Catenary	Parabolic
1 Bottom Level	1 Out-of-Plane	2.89	2.87
	2 In-Plane	3.24	3.22
	3 In-Plane	5.90	5.64
	4 Out-of-Plane	5.90	5.64
2	1 Out-of-Plane	1.96	1.94
	2 In-Plane	3.18	3.12
	3 In-Plane	3.99	3.79
	4 Out-of-Plane	3.99	3.80
3	1 Out-of-Plane	2.05	2.05
	2 In-Plane	2.62	2.59
	3 In-Plane	4.18	4.01
	4 Out-of-Plane	4.18	4.01
4	1 Out-of-Plane	2.02	2.01
	2 In-Plane	2.31	2.31
	3 In-Plane	3.95	4.10
	4 Out-of-Plane	3.95	4.10
5 Top Level	1 Out-of-Plane	1.44	1.41
	2 In-Plane	1.81	1.82
	3 In-Plane	2.82	2.89
	4 Out-of-Plane	2.83	2.90

Table 5.1: Natural frequencies of WTMJ guy cables.

The first four natural frequencies of guy cables at each of the five guy levels are presented in Table 5.1. As can be seen from the results, the cables that attach to the top of the mast (guy level 5) have the lowest natural frequencies. This is due to the fact that the cables considered have a relatively similar pre-tensioning and stiffness (cross-sectional area and elasticity), but lengths that vary significantly. Hence, as the ratio of AE/L decreases for a cable, so does its natural frequency (for constant tension). Another behavior, which was noted from the analysis, is that the second in-plane frequency (the first anti-symmetrical frequency) and the second out-of-plane frequency are almost identical. From Irvine (1981), the out-of-plane frequency of a cable was shown to be,

$$\omega_n = \frac{n\pi}{l} \left(\frac{H}{m} \right)^{1/2} \quad (5.1)$$

where $n = 1, 2, 3, \dots$

Similarly, Irvine (1981) showed that the anti-symmetric in-plane modes becomes,

$$\omega_n = \frac{2n\pi}{l} \left(\frac{H}{m} \right)^{1/2} \quad (5.2)$$

where $n = 1, 2, 3, \dots$. Hence, it can be seen from equations 5.1 and 5.2 that the second and fourth out-of-plane frequencies will correspond with the first and second anti-symmetric in-plane modes.

The results of an analysis of the WTMJ tower mast fixed at its base with no guy cable interaction are presented in Table 5.2. The analyses were conducted using the program developed during this study and the results were compared with the commercial software package SAP90™. The mast of WTMJ tower was represented by 45 three-dimensional beam elements. The software developed in this study has the ability to evaluate torsional vibration modes. However, as no torsional properties were available for the WTMJ tower, torsional vibration frequencies were not presented. As can be seen from Table 5.2, the results obtained from the present study and SAP90™ agree very closely when effect of self-weight was neglected (Appendix A). When the analysis was completed including the effects of self-weight, the results reflect the expected reduction in the first few natural frequencies (Przemieniecki 1968).

Excited Mode	Natural Frequency (rad/sec)		
	Present Study Self-Weight Neglected	SAP90™	Present Study Self-Weight Included
Z-Bending	0.4238	0.4234	0.2562
X-Bending	0.4238	0.4234	0.2562
Z-Bending	2.4886	2.4366	2.3894
X-Bending	2.4886	2.4366	2.3894
Z-Bending	3.6864	3.5879	3.5620
X-Bending	3.6864	3.5879	3.5620

Table 5.2: Natural frequencies of tower mast (fixed base) without guy cables.

Free vibration response of WTMJ tower was examined by including the interaction between guy cables and tower mast. A comparison of natural frequencies corresponding to a model that included the out-of-plane stiffness of the guy cables is presented in Table 5.3. The first two columns display the results obtained by Saxena (1988) using a parabolic profile and sixteen cable elements for each guy cable. Saxena used the analytical formulation presented by Veletsos and Darbe (1983) to derive the dynamic stiffness of a cable element. The analytical results (first column) follow the assumptions stated above for guy cables, while the mast of the tower was also modelled following an analytical approach. The third column in Table 5.3 presents the results obtained from this study using the program GTAP (Guyed Tower Analysis Program). For this case, the parabolic finite element developed in chapter 2 was used to model the cables. The guy cables were each modelled by eight cable elements with lumped mass idealization. The last two columns in Table 5.3 were also obtained using the GTAP software using catenary profile for cables, and lumped and consistent mass idealizations respectively. In the final column of Table 5.3, the vibration modes are identified as either an in-plane (I) or out-of-plane (O) for cable excitations, or as a bending vibration mode of the tower mast. The number following the type of excitation indicates the guy level.

Natural Frequency (rad/sec)					
Analytical Parabola Lumped	Saxena Parabola Lumped	GTAP Parabola Lumped	GTAP Catenary Lumped	GTAP Catenary Consistent	Excited Mode
1.37	1.39	1.36	1.32	1.34	I - 5
1.44	1.44	1.43	1.39	1.41	O - 5
1.47	1.47	1.46	1.42	1.44	O - 5
1.82	1.73	1.76	1.74	1.76	I - 5
1.95	1.93	1.95	1.94	1.96	O - 2
1.95	1.94	1.95	1.94	1.96	O - 2
2.03	2.03	2.04	1.99	2.02	O - 3
2.05	2.03	2.04	2.00	2.03	O - 3
2.05	2.04	2.05	2.02	2.04	O - 4
2.07	2.05	2.05	2.02	2.05	O - 4
2.14	2.12	2.15	2.12	2.15	I - 4
2.31	2.30	2.34	2.31	2.34	I - 4
-	-	2.36	2.36	2.37	Bending
2.45	2.43	2.46	2.44	2.47	I - 3

Table 5.3: WTMJ natural frequencies (out-of-plane stiffness included).

As can be seen from the results presented in Table 5.3, there was little discrepancy between various solutions corresponding to the different methods of analysis. The natural frequencies obtained from the different analysis methods were all within 4% of one another. Since the cable element used by Saxena and the parabolic element used in the GTAP program were developed using the same theory, the results for these approximations were almost identical.

Table 5.4 presents a comparison of the natural frequencies obtained for the WTMJ Tower when the out-of-plane stiffness of the guy cables was excluded. Again, the results obtained from parabolic cable model agree closely with the results from Saxena (1988). The present results show an in-plane cable excitation at guy level five (1.76 parabola and 1.74 and 1.76 catenary) which is missing from the results presented by McCaffrey (1969). The corresponding solution given by Saxena appeared to show what seems to be an out-of-plane mode near this frequency (1.73 Table 5.3). Furthermore, the present analysis identified a bending frequency of the mast near 2.37 rad/sec.

Natural Frequency (rad/sec)						
McCaffrey Parabola	McCaffrey Catenary	Saxena Parabola Lumped	GTAP Parabola Lumped	GTAP Catenary Lumped	GTAP Catenary Consistent	Excited Mode
1.39	1.44	1.39	1.40	1.37	1.34	I - 5
-	-	-	1.76	1.74	1.76	I - 5
2.14	2.17	2.12	2.15	2.12	2.19	I - 4
2.46	2.46	2.30	2.34	2.31	2.34	I - 4
-	-	-	2.37	2.37	2.38	Bending
2.81	2.78	2.43	2.46	2.45	2.47	I - 3

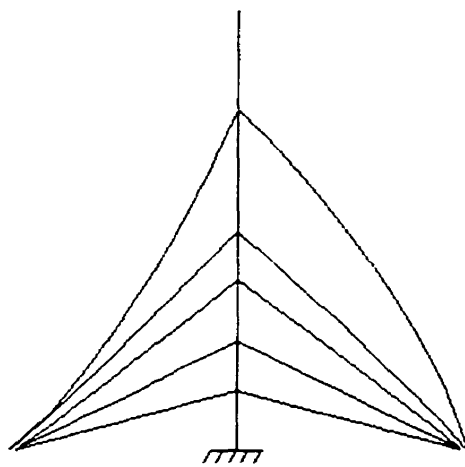
Table 5.4: WTMJ natural frequencies (out-of-plane stiffness neglected).

Examination of natural frequencies of individual guy cables (Table 5.1) and comparison with the results obtained for WTMJ tower (Table 5.3), indicates that the interaction between guy cables and tower mast have virtually no influence on the out-of-plane frequencies of the guys. Hence, the out-of-plane frequencies of cables attached to a tower may be estimated by a simple free vibration analysis of individual guy cables. However, as can be seen from the results, in-plane frequencies of individual cables cannot be used to estimate the in-plane frequencies of cables attached to a tower mast. For example, the first in-plane frequency of 1.40 rad/sec (Table 5.4) does not agree closely with the lowest in-plane frequency obtained from the analysis of individual cable. However, the second in-plane frequency (1.76, Table 5.4) does seem to coincide with the lowest in-plane frequency (1.82, Table 5.1) determined from the analysis of that cable. Based on the results, it was concluded that the cable elements have negligible coupling to the mast for out-of-plane frequencies. This however was not the case for in-plane frequencies. As in-plane frequencies appear in the tower which were independent from the in-plane frequencies obtained from the lone guy cable analyses, strong coupling exist between the tower and the in-plane DOF of cables.

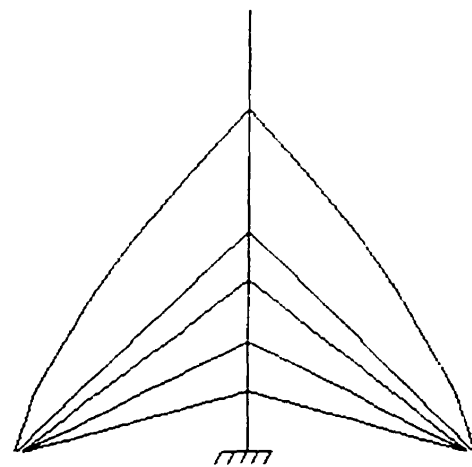
MODE SHAPES

The first twelve in-plane and bending modeshapes of the WTMJ tower are shown in Figure 5.1 (*a* to *l*). As expected, the longer cables (upper levels) are excited at frequencies which are lower in magnitude when compared with the shorter (lower level)

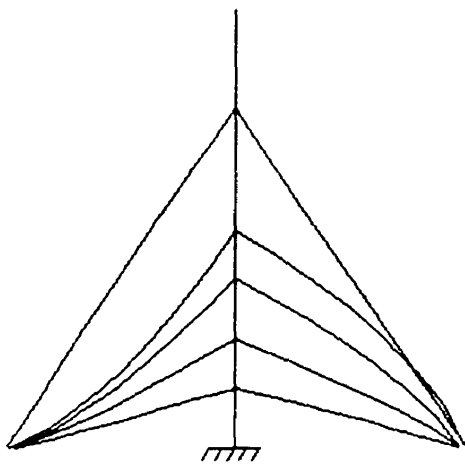
guy cables. Examining the modeshapes, it was observed that vibrations corresponding to 2.47 and 2.88 rad/sec (f & i) show relatively large motions at the uppermost portions of the mast in comparison to the remainder of the mast. This is in part due to the fact that the upper extremities of the mast have more freedom, as they are not laterally restrained by the guy cables like the lower portions of the mast. Furthermore, examination of tower properties revealed that the uppermost 25 meters of the tower mast correspond to an antenna of approximately 1/2000 of the stiffness of the lower portions of mast.



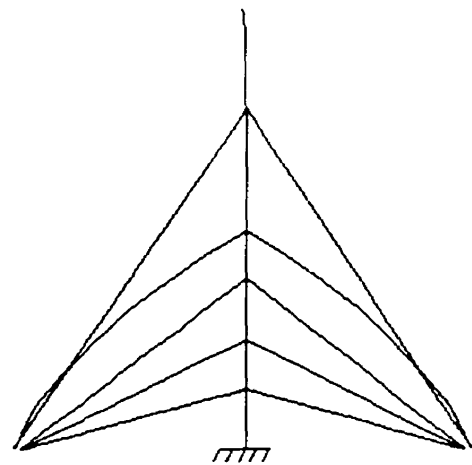
a) 1.34 rad/sec



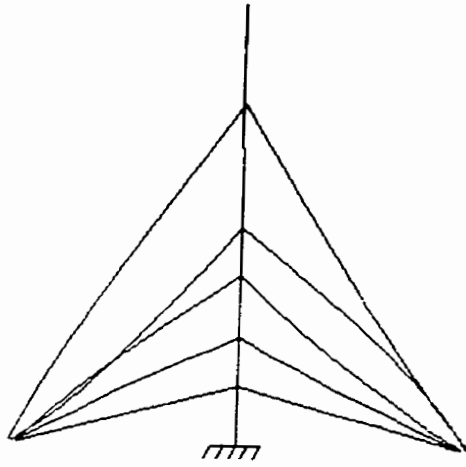
b) 1.76 rad/sec



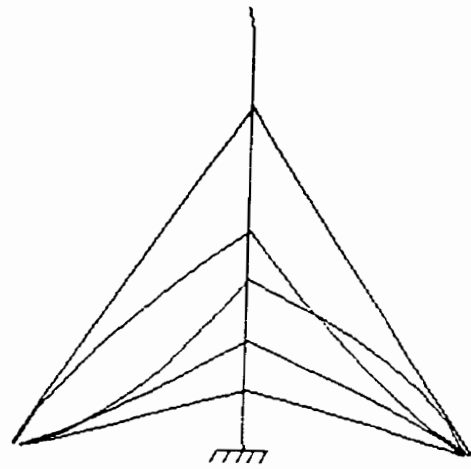
c) 2.15 rad/sec



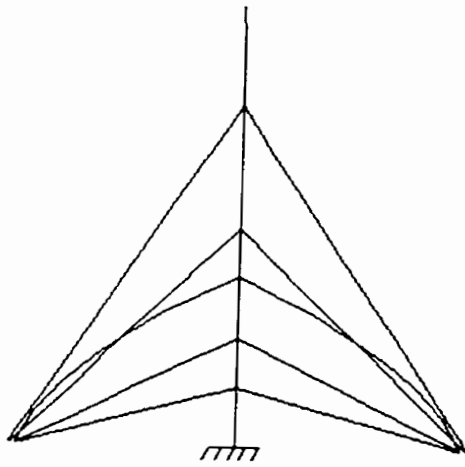
d) 2.34 rad/sec



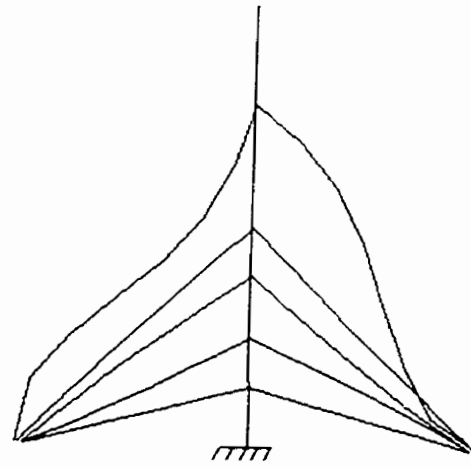
e) 2.37 rad/sec



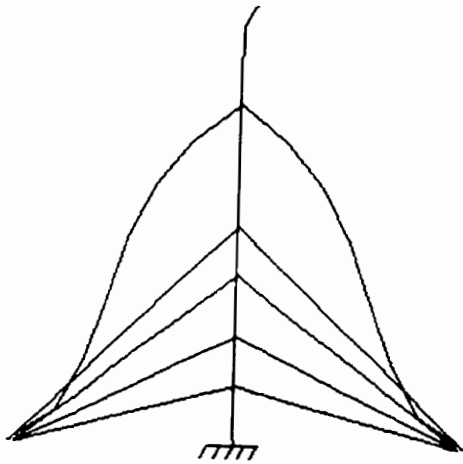
f) 2.47 rad/sec



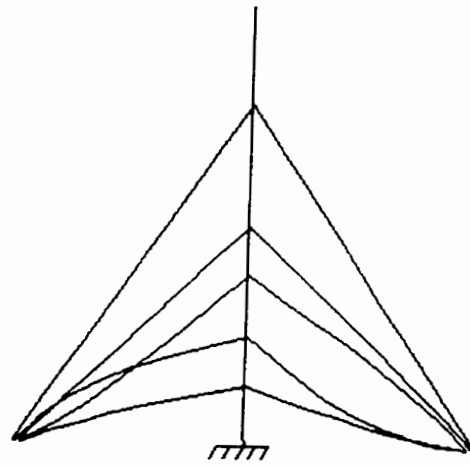
g) 2.61 rad/sec



h) 2.87 rad/sec



i) 2.88 rad/sec



j) 2.96 rad/sec

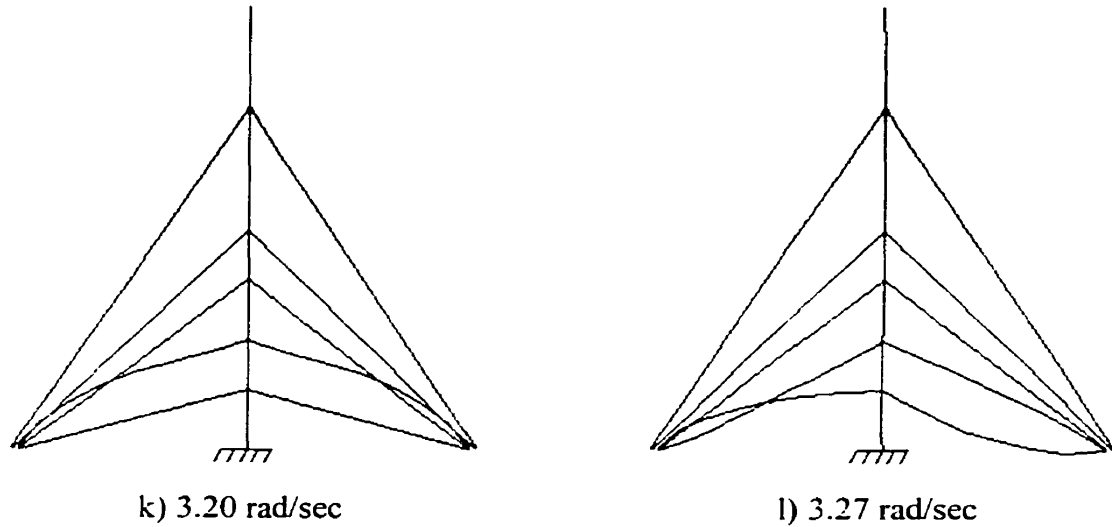


Figure 5.1: WTMJ tower modeshapes.

5.2 PARAMETRIC STUDY

TOWER MAST LACING PATTERNS

For the following parametric studies, two similar towers were considered, Tower A and Tower B. Both towers stand 145 m in height and have identical geometry and material properties with the exception that Tower B has three guy levels as opposed to Tower A which only has one level of guy cables. The material properties of Towers A and B are shown in Table 5.5, while the geometry of the towers is shown in Figures 5.2 and 5.3.

Material Property	Tower A	Tower B
Mast Elasticity	2.0E+011 Pa	2.0E+011 Pa
Cable Elasticity	1.65E+011 Pa	1.65E+011 Pa
Steel Density (for cables and mast)	8100 kg/m ³	8100 kg/m ³
Cable Tension	40,000 N	40,000 N
Cable Area	0.4E-003 m ²	0.4E-003 m ²

Table 5.5: Material properties of Towers A and B

Utilizing the software developed in this study, free vibration response of Towers A and B was determined. The guyed tower analysis was completed using eight cable elements for each guy cable and five different lacing patterns shown in Figure 2.6.

Table 5.6 presents the natural frequencies of Tower A for the five different lacing pattern configurations and the associated excitation mode. As Tower A features only one guy level, the excitation mode is defined as either an in-plane (I) or out-of-plane (O) for cable excitations. As can be seen from Table 5.6, the natural frequencies of the guyed tower system were generally consistent for the five different lacing patterns. Examination of the out-of-plane frequencies indicates that the maximum discrepancy between the five different lacing patterns was less than 0.5%. This behavior is consistent with that identified from the WTMJ tower which showed that the tower mast has virtually no influence on the out-of-plane vibrations of guy cables. However, two of the in-plane frequencies (the first and seventh) showed some variation in natural frequency for different lacing patterns. The maximum difference in natural frequency for these in-plane modes was in the order of about 10-12%, while the remaining in-plane frequencies showed virtually no change in natural frequency for the various lacing patterns. This behavior was also consistent with that from the WTMJ tower analysis that showed that only some in-plane frequencies show strong interaction between the tower mast and guy cables.

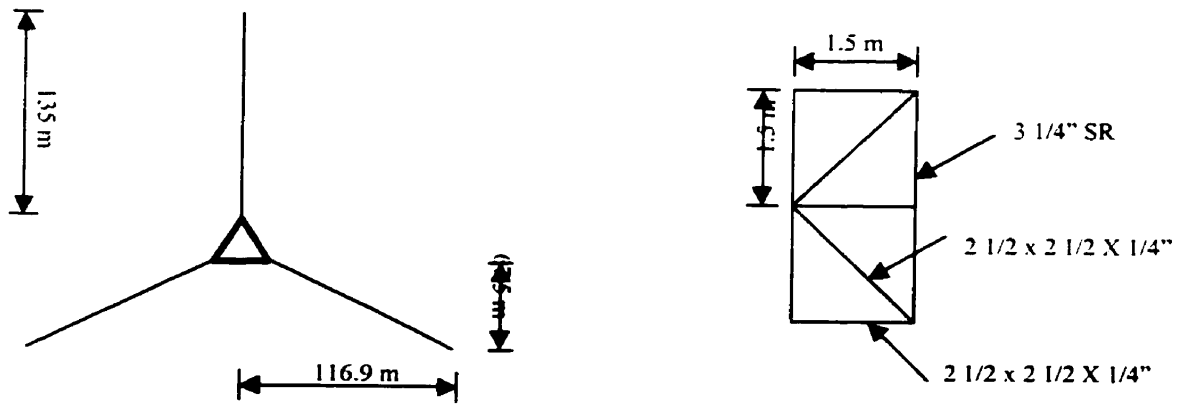
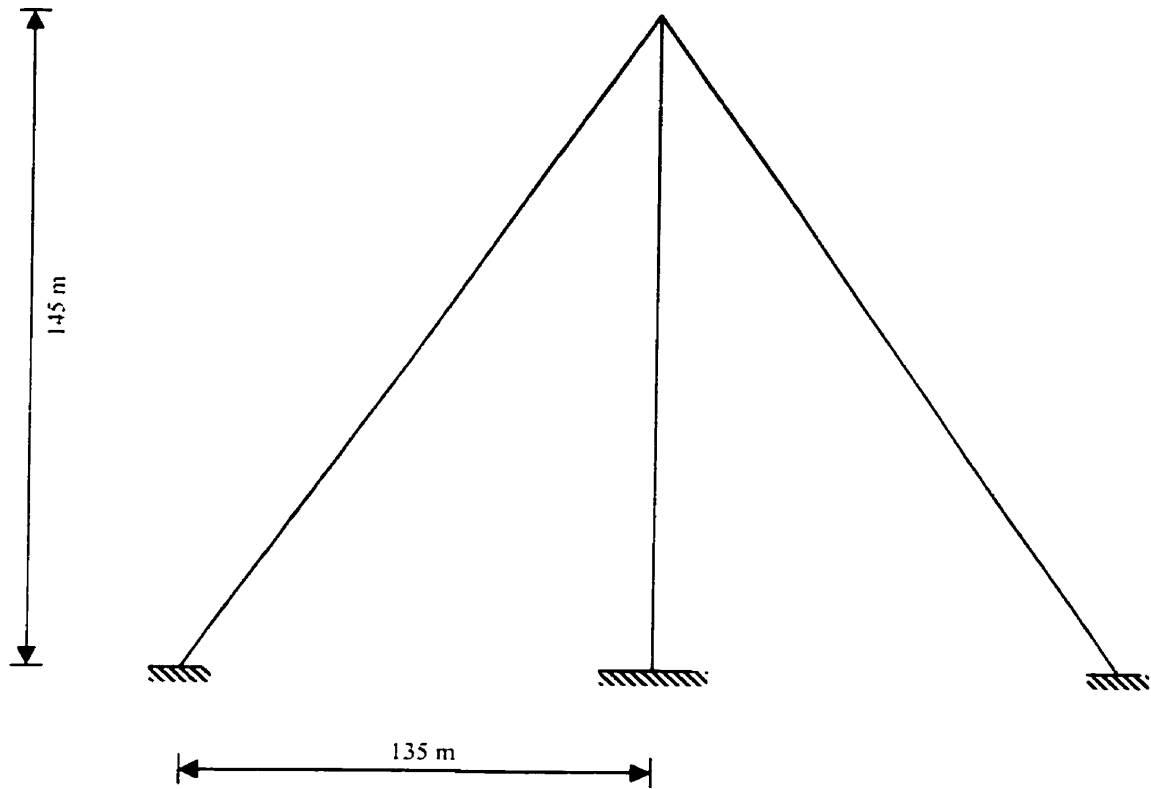


Figure 5.2: Geometry of Tower A.

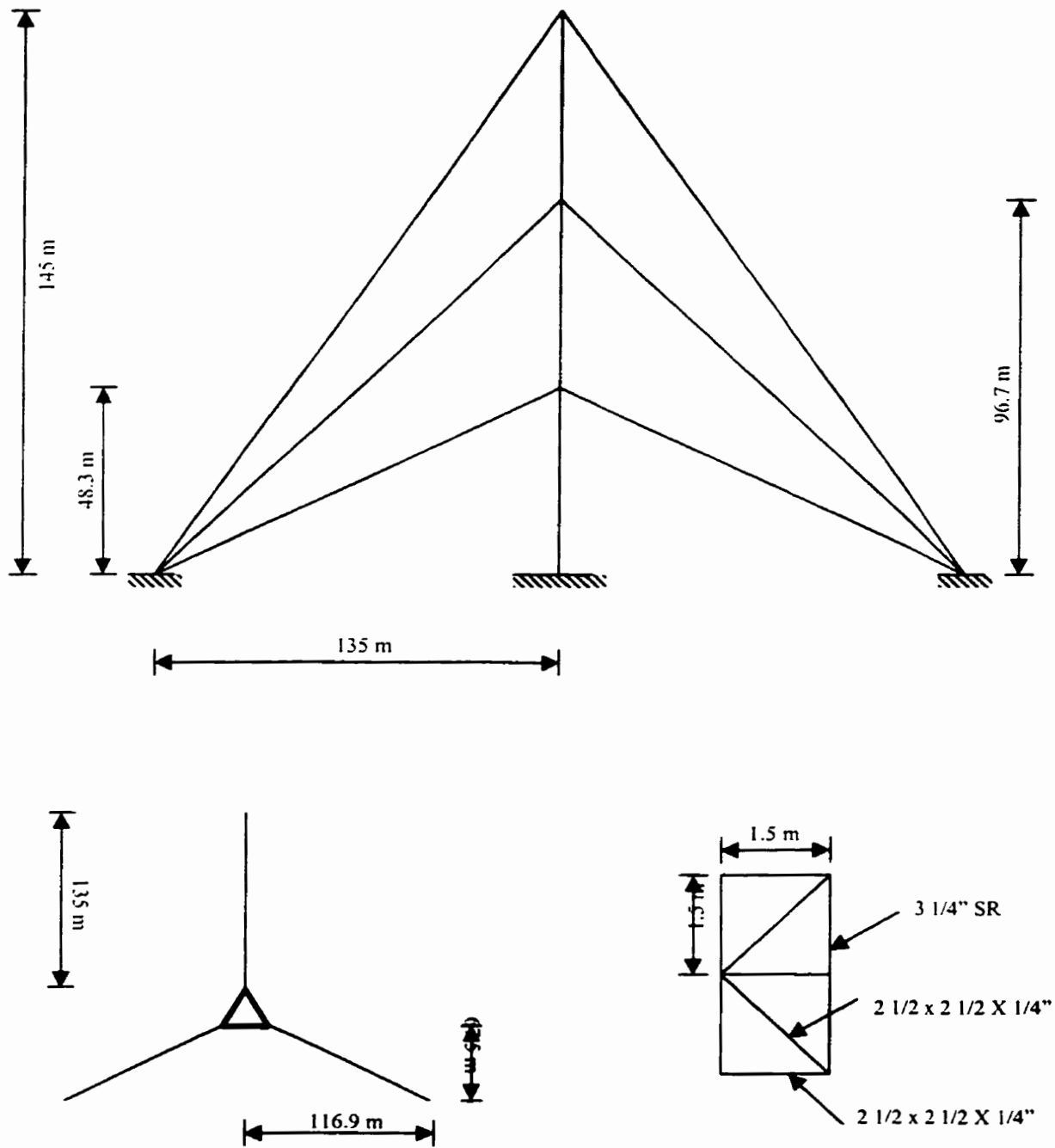


Figure 5.3: Geometry of Tower B.

Natural Frequencies (rad/sec)					
Pattern 1	Pattern 2	Pattern 3	Pattern 4	Pattern 5	Excited Mode
1.87	1.87	1.96	1.84	1.77	I
2.22	2.22	2.23	2.22	2.22	O
2.36	2.36	2.38	2.36	2.35	I
2.89	2.89	2.89	2.89	2.89	I
4.55	4.55	4.55	4.55	4.55	I
4.56	4.56	4.56	4.56	4.56	O
5.90	5.90	6.23	5.78	5.56	I

Table 5.6: Natural frequencies of Tower A for various lacing patterns.

Natural Frequencies (rad/sec)					
Pattern 1	Pattern 2	Pattern 3	Pattern 4	Pattern 5	Excited Mode
2.18	2.18	2.18	2.18	2.17	O-1
2.21	2.21	2.21	2.21	2.21	O-1
2.26	2.26	2.26	2.25	2.25	I-2
2.26	2.26	2.26	2.25	2.25	O-1
2.31	2.31	2.31	2.31	2.31	O-2
2.39	2.39	2.40	2.40	2.38	I-2
2.58	2.58	2.58	2.58	2.58	O-3
2.83	2.83	2.83	2.83	2.83	I-1
3.14	3.14	3.14	3.14	3.14	I-2
3.21	3.21	3.22	3.22	3.20	I-3
4.02	4.02	4.02	4.02	4.03	I-3
4.51	4.51	4.51	4.51	4.51	I-1

Table 5.7: Natural frequencies of Tower B for various lacing patterns.

A comparison of Figures 5.2 and 5.3 indicates that Tower B is essentially identical to Tower A with the exception that Tower B contains two additional levels of guy cables. Table 5.7 presents the first few natural frequencies for Tower B for the five different tower mast lacing patterns. A comparison of the natural frequencies for Towers A and B indicates that the variation of lacing pattern has virtually no influence on the observed natural frequencies of the guyed tower. Based on the previous observations, it was not expected that the tower mast would have any significant influence on the out-of-

plane frequencies. However, the tower mast also appeared to have no significant influence on any of the in-plane frequencies observed. The additional two guy levels on Tower B provide restraint of the tower mast at four points, while Tower A was only restrained at two points (top guy level and tower base). As such, it appears that the additional guy cables act to restrict the coupling of tower mast with the in plane DOFs. To further illustrate this point, Figures 5.4 and 5.5 show some selected mode shapes of Towers A and B respectively.

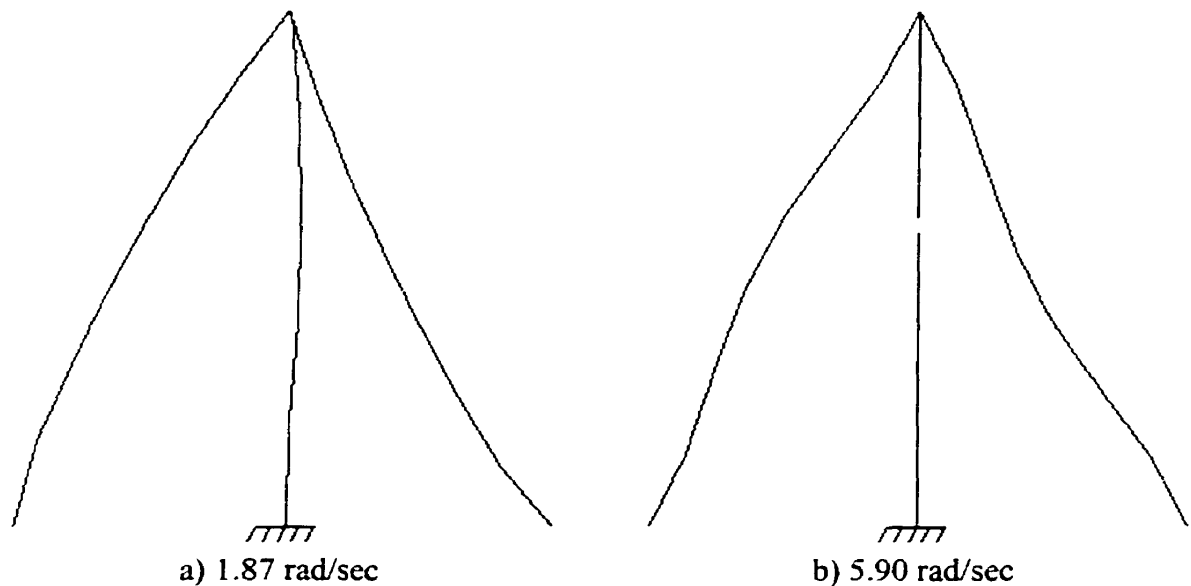


Figure 5.4: Selected modeshapes of Tower A (lacing pattern 1).

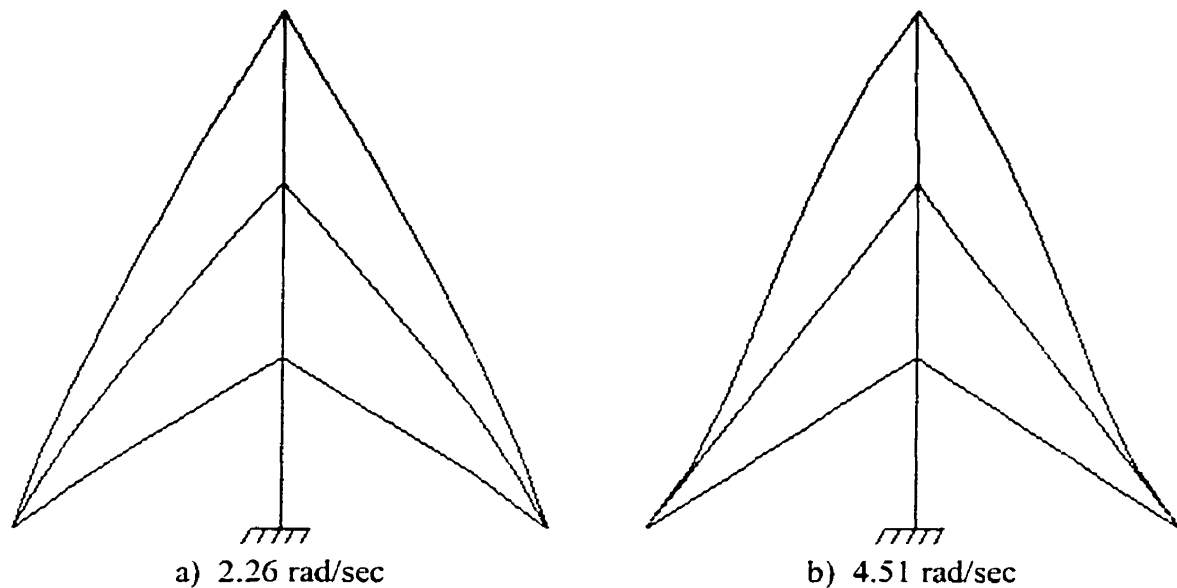


Figure 5.5: Selected modeshapes of Tower B (lacing pattern 1).

As can be seen from Figures 5.4 and 5.5, larger motions of the tower mast are noted for Tower A. The additional guy levels in Tower B act to increase the apparent stiffness of the tower mast that results in smaller overall deflections of the mast.

GUY CABLE TENSION

As it has been shown that a tower mast generally has little influence on the overall dynamic behavior of a guyed tower system, the influence of variations in guy cable tension on guyed tower systems is examined next. Consider Tower A subject to uniform sustained wind as shown in Figure 5.6. In this situation, the windward guy experiences an increased tensile force due to the applied wind load on the tower, while the cables on the leeward side experience a somewhat lower tension. For simplicity, it has been assumed that a guy cable perpendicular to the wind direction experiences no change in cable tension. The material and geometric properties for Tower A are as previously described, with the exception that the guy cable tensions were subject to fixed variation.

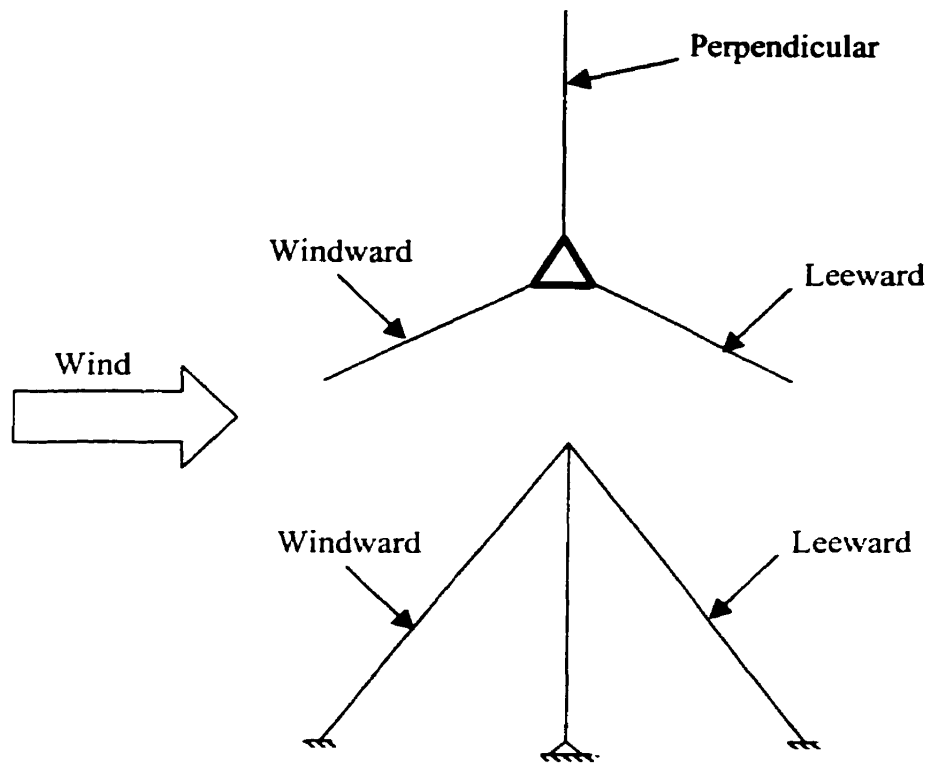


Figure 5.6: Tower A subjected to sustained uniform wind loading.

An analysis of Tower A was completed using the software developed in this study and considering variations in guy cable tensions in order to simulate the wind loading conditions previously described. The natural frequencies of Tower A, for a 10%, 30% and 50% variation in guy cable tension (i.e. windward guy tension increases, leeward guy tension decreases by an equal amount, and tension of guys perpendicular to wind remains at 40,000 N) have been shown in Table 5.8. For each corresponding frequency, the excited cable mode has been identified as either in-plane (I) or out-of-plane (O) as before. The guy cable is further identified as windward, leeward or perpendicular in Table 5.8. For comparison, an analysis of Tower A with no variation in cable tension (first column) has also been included in Table 5.8. Lacing pattern 5 was used for the mast of tower.

Natural Frequency (rad/sec)				Excited Mode	Excited Cable
0%	10%	30%	50%		
1.77	-	-	-	I	-
-	1.76	1.71	1.67	I	Leeward
-	1.78	1.80	1.80	I	Perpendicular
-	2.39	2.51	2.66	I	Windward
2.22	-	-	-	O	-
-	2.12	1.87	1.58	O	Leeward
-	2.22	2.20	2.21	O	Perpendicular
-	2.36	2.55	2.74	O	Windward
2.35	-	-	-	I	-
-	2.28	-	-	I	Leeward
-	2.36	-	-	I	Perpendicular
-	2.90	-	-	I	Windward
-	-	2.26	2.27	O	Perpendicular
-	-	2.97	3.14	I	Leeward
4.55	-	-	-	I	-
-	4.33	3.82	3.23	I	Leeward
-	4.55	4.56	4.56	I	Perpendicular
-	4.78	5.19	5.52	I	Windward
4.56	-	-	-	O	-
-	4.33	3.82	3.23	O	Leeward
-	4.56	4.56	4.56	O	Perpendicular
-	4.78	5.19	5.58	O	Windward

Table 5.8: Natural frequencies of Tower A for variations in cable tension.

The observed natural frequencies of the tower showed a consistent trend. Natural frequency of leeward guy was observed to decrease as a function of decreasing cable tension. The opposite was true for the windward guys, where the natural frequencies increase with increasing cable tension. These observations were consistent with the theory and results presented in Chapters 2 and 3, which showed that for a cable of identical material and geometric properties, the natural frequency is a function of cable tension. The natural frequency of the perpendicular guy (no change in cable tension) generally remained same as that of a tower not subjected to any change in guy tension. However, a minor variation in the natural frequency (0 to 2%) was noted for the perpendicular cable. While difficult to confirm, it is anticipated that these minor frequency fluctuations were related to the structural interaction of three guy cables and tower mast. For higher cable tension variations (30% and 50%), new in-plane and out-of-

plane frequencies emerged. These frequencies naturally arise as a result of the large difference in cable tension between the guy cables at the same level.

Chapter 6

CONCLUSIONS

A finite element based methodology was successfully applied to determine natural frequencies and mode shapes of guyed towers. The guyed tower model consists of three main components, the guy cables, tower mast and torsion arms. By applying the finite element method to a three-dimensional cable element following a catenary or parabolic profile, element stiffness and mass matrices were derived. Using a three-dimensional beam-column element that accounts for five different lacing patterns, stiffness and mass matrices for the tower mast were computed. The global mass and stiffness matrices were used in an eigen analysis to determine the natural frequencies and modeshapes of the guyed tower system. With the ease of programming the finite element method on a personal computer, an interactive software package was developed to complete a free vibration analysis of guyed towers. The software included a user friendly graphical user interface. The graphical user interface provides several options in terms of tower geometry and properties and also displays the tower modeshapes.

To verify the validity of the numerical model developed in this study, several comparisons were made with existing solutions for a single cable, a cantilever beam and guyed towers. The comparisons showed good agreement with existing solutions and confirmed the validity of the structural model. From the numerical studies, several conclusions were drawn.

The natural frequencies of a single guy cable were found to be a function of the cable pre-tension force and stiffness. For a given cable stiffness, the natural frequency

was shown to increase with increasing cable tension. Furthermore, for constant cable tension, the cable frequency was observed to decrease with increasing cable length. A comparison between lumped and consistent mass idealizations showed that the rate of convergence was only slightly faster for the consistent mass representation. Even though the cable element derived in this study was much simpler, it compared favourably with an existing fully non-linear solution. It was also shown that the equivalent elasticity approach based on a straight chord produced reasonable results for out-of-plane cable frequencies only.

Several analyses were completed which examined the behaviour of the individual guy cables, tower mast and complete guyed tower systems. Based on a comparison of natural frequencies of individual guy cables and those attached to a tower, it was found that interaction between the tower mast and guy cables has virtually no influence on the out-of-plane frequencies of guy cables. However, the in-plane frequencies showed strong influence due to coupling of the guy cables and the tower mast.

Guyed towers are generally very tall. As a result, the self-weight of tower imposes a considerable axial load on the lower portion of tower mast. It was found that the tower self-weight affects the first few natural frequencies of a tower mast. As such, self-weight effects were considered in the analysis.

Parametric studies were completed to examine the influence of tower lacing pattern, guy cable tension and guy configuration on the dynamic behaviour of a guyed tower. These parametric studies showed that tower lacing patterns generally had little effect (up to 10% variation) on the natural frequencies of a guyed tower system. Furthermore, the effect of lacing patterns on the in-plane natural frequencies was found to decrease as the number of guy levels increased. Natural frequencies of a guyed tower were found to change significantly when variations in guy tensions were included in the analysis. For example, 30-50% variations in leeward and windward guys of tower resulted in new in plane vibration modes. Windward cables experienced increase in natural frequencies whereas leeward cable frequencies were decreased.

While a free vibration analysis is a good starting point to understand dynamic behaviour of guyed towers, there are instances where a forced vibration analysis is

required. As such, the present software was developed such that it could be extended to consider forced vibration problems by means of the modal superposition method.

REFERENCES

- Bathe, K-J. (1982). Finite Element Procedures in Engineering Analysis. Prentice-Hall, Inc.
- Chopra, A. K. (1995). Dynamics of Structures. Prentice-Hall, Inc.
- Clough, R.W., and Penzien, J. (1975). Dynamics of Structures. McGraw-Hill, Inc.
- Cohen, E., and Perrin, H. (1957a). "Design of Multi-leveled Guyed Towers: Wind Loading." *Journal of the Structural Division*, ASCE, 83, Paper Number 1355.
- Cohen, E., and Perrin, H. (1957b). "Design of Multi-leveled Guyed Towers: Structural Analysis." *Journal of the Structural Division*, ASCE, 83, Paper Number 1356.
- Craig, R.R. (1981). Structural Dynamics. John Wiley & Sons, Inc.
- Davenport, A.G. (1959). "The Wind Induced Vibration of Guyed and Self Supporting Cylindrical Columns." *Transactions, Engineering Institute of Canada*, 3, 119-141.
- Davenport, A.G. and Steels, G.N. (1965). "Dynamic Behavior of Massive Guy Cables." *Journal of the Structural Division*, ASCE, 91, ST2, Proceedings Paper 4293, 43-70.
- Dean , D.L. (1961). "Static and Dynamic Analysis of Guy Cables." *Journal of the Structural Division*, ASCE, 87, 1-21.
- Dean , D.L. (1962). "Static and Dynamic Analysis of Guy Cables." *Transactions*, ASCE, 127, part II, 382-402.
- Ekhande, S.G., and Madugula, M.K.S. (1988). "Geometric Non-linear Analysis of Three-dimensional Guyed Towers." *Computers and Structures*, 29, 801-806.
- Fleming, J.F. (1979). "Nonlinear Static Analysis of Cable-Stayed Bridge Structures." *Computers and Structures*, 10, 621-635.

Goldberg, J.E., and Meyers, V.J. (1965). "A Study of Guyed Towers." *Journal of the Structural Division*, ASCE, 91, 57-76.

Goldberg, J.E., and Gaunt, T.J. (1973). "Stability of Guyed Towers." *Journal of the Structural Division*, ASCE, 99, 741-756.

Harrison, H.B. (1973). Computer Methods in Structural Analysis. Prentice-Hall, Inc.

Henghold, W.M., and Russell, J.J. (1976). "Equilibrium and Natural Frequencies of Cable Structures (A Nonlinear Finite Element Approach)." *Computers and Structures*, 6, 267-271.

Henghold, W.M., and Russell, J.J., and Morgan, D.M. (1977). "Free Vibrations of Cable in Three Dimensions." *Journal of the Structural Division*, ASCE, 103, 1127-1136.

Hull, F.H. (1962). "Stability Analysis of Multi-Level Guyed Towers." *Journal of the Structural Division*, ASCE, 88, 61-80.

Inman, D.J. (1996). Engineering Vibration. Prentice-Hall, Inc.

Irvine, H.M. and Caughey, T.K. (1974). "The Linear Theory of Free Vibrations of a Suspended Cable." *Proceedings of the Royal Society*, London, England, Series A, 341, 299-315.

Irvine, H.M. (1978). "Free Vibrations of Inclined Cables." *Journal of the Structural Division*, ASCE, 104, 343-347

Irvine, H.M. (1981). Cable Structures. MIT Press.

Kahla, N.B. (1993). "Static and Dynamic Analysis of Guyed Towers." A thesis submitted to the Faculty of Graduate school, University of Wisconsin at Madison, in partial fulfillment of the requirements for the degree of Doctor of Philosophy.

Logan, D.L. (1992). A First Course in the Finite Element Method. PWS-KENT Publishing Company, 2nd ed.

McCaffrey, R.J. (1969). "Dynamics of Guyed Towers." A thesis submitted to the faculty of graduate school, Marquette University at Milwaukee, in partial fulfillment of the requirements for the degree of Master of Science.

McCaffrey, R.J., and Hartmann, A.J. (1972). "Dynamics of Guyed Towers." *Journal of the Structural Division*, ASCE, 98, 1309-1323

Martin, R.S., and J.W. Wilkinson (1968), Reduction of the symmetric eigenproblem $Az = \lambda Bz$ and related problems to standard form, *Numerische Mathematik*, 11, 99-119.

Mathur, R.K. (1985). "Structural Dynamic Characteristics of Transmission Systems." A thesis submitted to the Faculty of Graduate studies, University of Manitoba at Winnipeg, in partial fulfillment of the requirements for the degree of Master of Science.

Miklofsky, H.A., and Abegg, M.G. (1966). "Design of Guyed Towers by Interaction Diagrams." *Journal of the Structural Division*, ASCE, 92, 245-256.

Nordien, J. (1986). "Hydro Tower Analysis Program." A thesis submitted to the Faculty of Graduate studies, University of Manitoba at Winnipeg, in partial fulfillment of the requirements for the degree of Master of Science.

Novak, M., and Davenport, A.G., and Tanaka, H. (1978). "Vibration of Towers due to Galloping of Iced Cables." *Journal of Engineering Mechanics*, ASCE, 104, 457-473

O'Brian, W.T. (1967). "General Solution of Suspended Cable Problems." *Journal of the Structural Division*, ASCE, 93, 1-26.

Odley, E.G. (1966). "Analysis of High Guyed Towers." *Journal of the Structural Division*, ASCE, 92, 160-190.

Peyrot, A.H., and Goulois, A.M. (1979). "Analysis of Cable Structures." *Computers and Structures*, 10, 805-813.

Przemieniecki, J.S. (1968). Theory of Matrix Structural Analysis. McGraw-Hill, Inc.

Romstad, K.M., and Chiesa, M. (1977). "Approximate Analysis of Guyed Towers." *Proceedings ASCE*, San Francisco, CA.

Rowe, R.S. (1958). "Amplification of Stress and Displacement in Guyed Towers." *Journal of the Structural Division*, ASCE, 84, Proceedings Paper 1821.

Saxena, R. (1988). "Free-Vibration Analysis of Guyed Structures." A thesis submitted to the Faculty of Graduate studies, University of Manitoba at Winnipeg, in partial fulfillment of the requirements for the degree of Master of Science.

Tong, P., and Pian, T.H.H., and Bucciarelli, L.L. (1971). "Mode Shapes and Frequencies by Finite Element Method using Consistent and Lumped Masses." *Computers and Structures*, 1, 623-638.

Veletsos, A.S. and Darbre, G.R. (1983). "Dynamic Stiffness of Parabolic Cables." *Earthquake Engineering and Structural Dynamics*, 11, 367-401.

West, H.H., Gerschwinder, L.F. and Suhoski, J.E. (1975). "Natural Vibrations of Suspended Cables." *Journal of the Structural Division*, ASCE, ST11, Proceedings Paper 11712, 2277-2291.

Williamson, R.A., and Margolin, M.N. (1966). "Shear Effects in Design of Guyed Towers." *Journal of the Structural Division*, ASCE, 92, 213-233.

Zienkiewicz and Taylor (1989). The Finite Element Method. Volumes 1 and 2, McGraw-Hill, Inc.

Nomenclature

E_{eq} - Equivalent modulus of elasticity.

E_c - Cable modulus of elasticity.

w - Cable unit weight.

A_c - Cable cross-sectional area.

L_p - Projected length of cable.

T - Cable tension.

L_c - Cable chord length.

d - Cable sag.

H - Horizontal component of cable tension.

q - Distributed self-weight of cable.

l - Horizontal component of cable length.

L_e - Effective cable length.

E - Modulus of elasticity for mast.

EA - Equivalent axial stiffness of tower mast.

EI - Equivalent flexural stiffness of tower mast.

GA - Equivalent shear stiffness of tower mast.

GJ - Equivalent torsional stiffness of tower mast.

ω - Natural frequency (rad/sec).

Ω - non-dimensionalized natural frequency.

Appendix

THREE-DIMENSIONAL CABLE ELEMENT

The local cable coordinate system was defined by considering the x_l axis in the plane of the cable along its length. The cable plane represents the plane that passes through the end points of the cable and tower base. Figure A.1 shows the cable plane. The y_l axis is also orientated in this plane and is perpendicular to the x_l axis. The z_l axis is perpendicular to the plane of the cable. Figure A.1 identifies the local and global axes of the cable.

The cable element considered for this study is shown in Figure 2.2. From equation 2.19 the elastic stiffness matrix $[K_E]$ for the three-dimensional cable (truss) element is

$$[K_E] = \frac{EA}{L} \begin{bmatrix} 1 & -1 \\ -1 & 1 \end{bmatrix} \quad (\text{A.1})$$

where E is the modified modulus of elasticity of the cable, A is the cross-sectional area of the cable element, L is the length of the element and T_0 is the pre-tension force applied to the guy cable with a nodal degree of freedom vector $\{d\} = \{u_1 \ u_2\}^T$.

Similarly, using equation 2.20 the stress stiffness matrix $[K_G]$ for the cable element under tension T_0 may be expanded as

$$[K_G] = \frac{T_0}{L} \begin{bmatrix} 1 & 0 & 0 & -1 & 0 & 0 \\ 0 & 1 & 0 & 0 & -1 & 0 \\ 0 & 0 & 1 & 0 & 0 & -1 \\ -1 & 0 & 0 & 1 & 0 & 0 \\ 0 & -1 & 0 & 0 & 1 & 0 \\ 0 & 0 & -1 & 0 & 0 & 1 \end{bmatrix} \quad (\text{A.2})$$

with a nodal degree of freedom vector $\{\delta\} = \{u_1 \ v_1 \ w_1 \ u_2 \ v_2 \ w_2\}^T$.

The total stiffness matrix of the cable element shown in Figure 2.2 was obtained by adding the elastic stiffness and stress stiffness matrices given above.

Figure A.1 shows the three points used to define the cable plane. The equation of the plane (n) may be expressed as,

$$n = (\mathbf{q} - \mathbf{p}) \times (\mathbf{r} - \mathbf{p}). \quad (\text{A.3})$$

From the equation of the plane, the unit vector perpendicular to this plane may be determined using linear algebra. By definition, this unit vector is one of the vectors to be used in the transformation. A second unit vector may be determined along the length of the cable. The final vector may be obtained by evaluating the cross product of the above two unit vectors. Hence, the unit vectors take the form of,

$$\begin{aligned} \hat{d}_x &= C_{xx}d_x + C_{xy}d_y + C_{xz}d_z \\ \hat{d}_y &= C_{yx}d_x + C_{yy}d_y + C_{yz}d_z \\ \hat{d}_z &= C_{zx}d_x + C_{zy}d_y + C_{zz}d_z. \end{aligned} \quad (\text{A.4})$$

From the above, the transformation matrix from the local to the global coordinate system is,

$$[T] = \begin{bmatrix} C_{xx} & C_{xy} & C_{xz} & 0 & 0 & 0 \\ C_{yx} & C_{yy} & C_{yz} & 0 & 0 & 0 \\ C_{zx} & C_{zy} & C_{zz} & 0 & 0 & 0 \\ 0 & 0 & 0 & C_{xx} & C_{xy} & C_{xz} \\ 0 & 0 & 0 & C_{yx} & C_{yy} & C_{yz} \\ 0 & 0 & 0 & C_{zx} & C_{zy} & C_{zz} \end{bmatrix} \quad (\text{A.5})$$

and $[K_G] = [T]^T [k] [T]$ (A.6)

where $[K_G]$ is the stiffness matrix with respect to the global coordinate system.

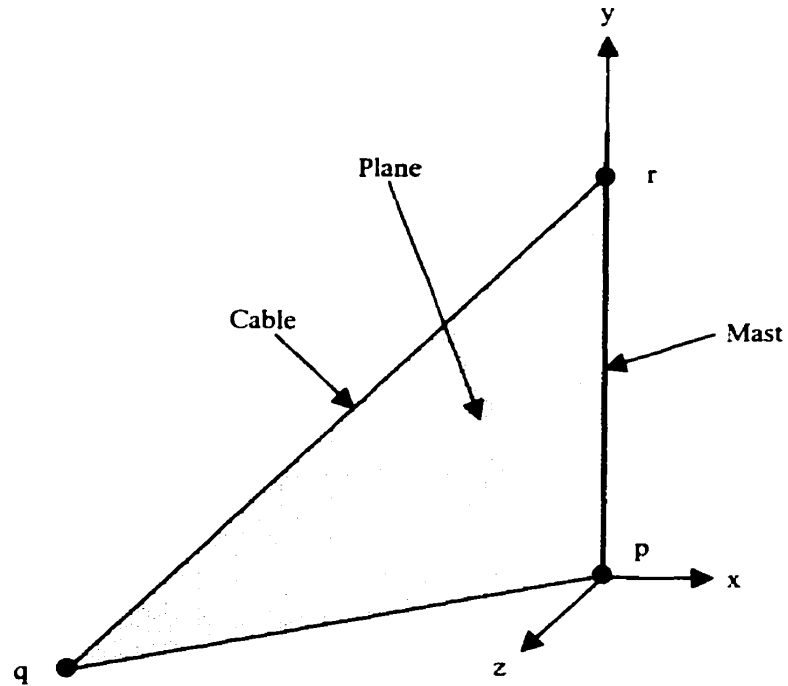


Figure A.1: Plane of a cable.

THREE-DIMENSIONAL BEAM ELEMENT

The local mass and stiffness matrices for a three-dimensional beam element were obtained by considering the axial, bending and torsional deformations of an element. This results in a beam element with six DOF (degrees of freedom) at each node (three translations and three rotations).

The local frame of reference and the displacement coordinates for a uniform three-dimensional beam element are shown below in Figure A.2. The stiffness and mass matrices for this beam element were obtained from the axial, bending, and torsion elements discussed by Craig (1981). The x -axis was taken along the centroidal axis of the cross-section and the y and z axes are principle axes in the cross-section. I_y and I_z are the moments of inertia along the y and z axes respectively and I_p is the polar moment of inertia about the x -axis.

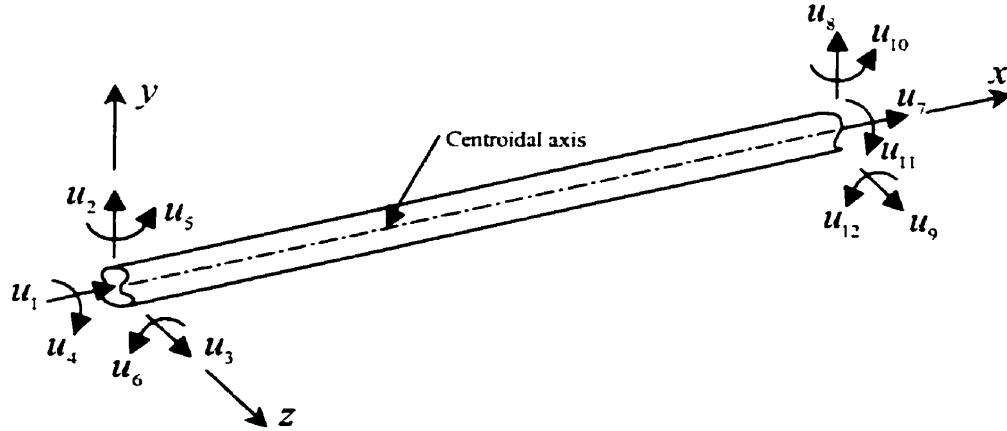


Figure A.2: Notation for a three-dimensional beam element.

For the beam element shown in Figure A.2, stiffness matrix is given by Craig (1981) as

$$[K] = \begin{bmatrix} \frac{EA}{L} & 0 & 0 & 0 & 0 & 0 & -\frac{EA}{L} & 0 & 0 & 0 & 0 & 0 \\ 0 & \frac{12EI}{L^3} & 0 & 0 & 0 & \frac{6EI}{L^2} & 0 & -\frac{12EI}{L^3} & 0 & 0 & 0 & \frac{6EI}{L^2} \\ 0 & 0 & \frac{12EI}{L^3} & 0 & -\frac{6EI}{L^2} & 0 & 0 & 0 & -\frac{12EI}{L^3} & 0 & -\frac{6EI}{L^2} & 0 \\ 0 & 0 & 0 & \frac{GJ}{L} & 0 & 0 & 0 & 0 & 0 & -\frac{GJ}{L} & 0 & 0 \\ 0 & 0 & -\frac{6EI}{L^2} & 0 & \frac{4EI}{L} & 0 & 0 & \frac{6EI}{L^2} & 0 & \frac{2EI}{L} & 0 & 0 \\ 0 & \frac{6EI}{L^2} & 0 & 0 & 0 & \frac{4EI}{L} & 0 & -\frac{6EI}{L^2} & 0 & 0 & \frac{2EI}{L} & 0 \\ -\frac{EA}{L} & 0 & 0 & 0 & 0 & 0 & \frac{EA}{L} & 0 & 0 & 0 & 0 & 0 \\ 0 & 0 & 0 & 0 & 0 & 0 & 0 & \frac{12EI}{L^3} & 0 & 0 & 0 & -\frac{6EI}{L^2} \\ 0 & 0 & 0 & 0 & 0 & 0 & 0 & 0 & \frac{12EI}{L^3} & 0 & \frac{6EI}{L^2} & 0 \\ 0 & 0 & 0 & -\frac{GJ}{L} & 0 & 0 & 0 & 0 & 0 & \frac{GJ}{L} & 0 & 0 \\ 0 & 0 & 0 & 0 & \frac{4EI}{L} & 0 & 0 & 0 & 0 & 0 & \frac{4EI}{L} & 0 \\ 0 & 0 & 0 & 0 & 0 & 0 & 0 & -\frac{6EI}{L^2} & 0 & 0 & 0 & \frac{4EI}{L} \end{bmatrix} \quad (A.7)$$

where \$E\$ is the Young's modulus of elasticity, \$GJ\$ is the torsional stiffness, \$L\$ is the length of the beam element and \$A\$ is the cross-sectional area of the beam element.

Craig (1981) also presented the consistent symmetric mass matrix for the beam element in Figure A.2

$$[M] = \frac{mL}{420} \begin{bmatrix} 140 & 0 & 0 & 0 & 0 & 0 & 70 & 0 & 0 & 0 & 0 & 0 \\ & 156 & 0 & 0 & 0 & 22L & 0 & 54 & 0 & 0 & 0 & -13L \\ & & 156 & 0 & -22L & 0 & 0 & 0 & 54 & 0 & 13L & 0 \\ & & & \frac{140I_p}{A} & 0 & 0 & 0 & 0 & 0 & \frac{70I_p}{A} & 0 & 0 \\ & & & & 4L^2 & 0 & 0 & 0 & -13L & 0 & -3L^2 & 0 \\ & & & & & 4L^2 & 0 & 13L & 0 & 0 & 0 & -3L \\ & & & & & & 140 & 0 & 0 & 0 & 0 & 0 \\ & & & & & & & 156 & 0 & 0 & 0 & -22L \\ & & & & & & & & 156 & 0 & 22L & 0 \\ & & & & & & & & & \frac{140I_p}{A} & 0 & 0 \\ & & & & & & & & & & 4L^2 & 0 \\ & & & & & & & & & & & 4L^2 \end{bmatrix} \quad (A.8)$$

where m is the mass per unit length of the element.

For the beam element shown in Figure A.2, Przemieniecki (1968) presented the representative stiffness matrix which included the effects of shear deformations as:

$$[K] = \begin{bmatrix} \frac{EA}{L} & 0 & 0 & 0 & 0 & 0 & -\frac{EA}{L} & 0 & 0 & 0 & 0 & 0 \\ & \frac{12EI_z}{L^3(1+\Phi_z)} & 0 & 0 & 0 & \frac{6EI_z}{L^2(1+\Phi_z)} & 0 & \frac{-12EI_z}{L^3(1+\Phi_z)} & 0 & 0 & 0 & \frac{6EI_z}{L^2(1+\Phi_z)} \\ & & \frac{12EI_z}{L^3(1+\Phi_z)} & 0 & \frac{-6EI_z}{L^2(1+\Phi_z)} & 0 & 0 & 0 & \frac{-12EI_z}{L^3(1+\Phi_z)} & 0 & \frac{-6EI_z}{L^2(1+\Phi_z)} & 0 \\ & & & \frac{GJ}{L} & 0 & 0 & 0 & 0 & 0 & \frac{-GJ}{L} & 0 & 0 \\ & & & & \frac{(4+\Phi_z)EI_z}{L(1+\Phi_z)} & 0 & 0 & 0 & \frac{6EI_z}{L^2(1+\Phi_z)} & 0 & \frac{(2-\Phi_z)EI_z}{L} & 0 \\ & & & & & \frac{(4+\Phi_z)EI_z}{L(1+\Phi_z)} & 0 & \frac{-6EI_z}{L^2(1+\Phi_z)} & 0 & 0 & 0 & \frac{(2-\Phi_z)EI_z}{L(1+\Phi_z)} \\ & & & & & & \frac{EA}{L} & 0 & 0 & 0 & 0 & 0 \\ & & & & & & & \frac{12EI_z}{L^3(1+\Phi_z)} & 0 & 0 & 0 & \frac{-6EI_z}{L^2(1+\Phi_z)} \\ & & & & & & & & \frac{12EI_z}{L^3(1+\Phi_z)} & 0 & \frac{6EI_z}{L^2(1+\Phi_z)} & 0 \\ & & & & & & & & & \frac{GJ}{L} & 0 & 0 \\ & & & & & & & & & & \frac{(4+\Phi_z)EI_z}{L(1+\Phi_z)} & 0 \\ & & & & & & & & & & & \frac{(4+\Phi_z)EI_z}{L(1+\Phi_z)} \end{bmatrix} \quad (A.9)$$

where $\Phi = \frac{12EI}{GA_s L^2}$.

Przemieniecki (1968) also presented the consistent symmetric mass matrix which included shear deformations for the beam element in Figure A.2 as:

$$[M] = mL$$

$$\begin{bmatrix} \frac{1}{3} & 0 & 0 & 0 & 0 & 0 & \frac{1}{6} & 0 & 0 & 0 & 0 & 0 \\ \frac{13}{35} + \frac{6I_p}{5AL^2} & 0 & 0 & 0 & \frac{11L}{210} + \frac{I_p}{10AL} & 0 & \frac{9}{70} + \frac{6I_p}{5AL^2} & 0 & 0 & 0 & \frac{13L}{420} + \frac{I_p}{10AL} \\ \frac{13}{35} + \frac{6I_p}{5AL^2} & 0 & -\frac{11L}{210} - \frac{I_p}{10AL} & 0 & 0 & 0 & \frac{9}{70} - \frac{6I_p}{5AL^2} & 0 & \frac{13L}{420} - \frac{I_p}{10AL} & 0 & 0 \\ \frac{I_p}{3A} & 0 & 0 & 0 & 0 & 0 & 0 & \frac{I_p}{6A} & 0 & 0 & 0 \\ \frac{L^2}{105} + \frac{2I_p}{15A} & 0 & 0 & 0 & 0 & 0 & -\frac{13}{35} + \frac{6I_p}{5AL^2} & 0 & -\frac{L^2}{140} - \frac{I_p}{30A} & 0 & 0 \\ \frac{L^2}{105} + \frac{2I_p}{15A} & 0 & \frac{13L}{420} - \frac{I_p}{10AL} & 0 & 0 & 0 & 0 & 0 & 0 & -\frac{L^2}{140} - \frac{I_p}{30A} & 0 \\ \frac{1}{3} & 0 & 0 & 0 & 0 & \frac{1}{3} & 0 & 0 & 0 & 0 & 0 \\ \frac{13}{35} + \frac{6I_p}{5AL^2} & 0 & 0 & 0 & 0 & \frac{13}{35} + \frac{6I_p}{5AL^2} & 0 & 0 & 0 & -\frac{11L}{210} + \frac{I_p}{10AL} & 0 \\ \text{sym.} & & & & & & & & \frac{13}{35} + \frac{6I_p}{5AL^2} & 0 & \frac{11L}{210} + \frac{I_p}{10AL} \\ & & & & & & & & \frac{I_p}{3A} & 0 & 0 \\ & & & & & & & & \frac{L^2}{105} + \frac{2I_p}{15A} & 0 & 0 \\ & & & & & & & & \frac{L^2}{105} + \frac{2I_p}{15A} & 0 & \frac{L^2}{105} + \frac{2I_p}{15A} \end{bmatrix}$$

(A.10)

The geometric stiffness matrix due to an axial load on the member was given by Przemieniecki (1968) as

$$[K_{ax}]_z = P \begin{bmatrix} \frac{6}{5L} & \frac{1}{10} & -\frac{6}{5L} & \frac{1}{10} \\ \frac{2L}{15} & \frac{1}{10} & -\frac{L}{30} & -\frac{L}{30} \\ \text{sym.} & \frac{6}{5L} & -\frac{1}{10} & \frac{2L}{15} \end{bmatrix} \quad (\text{A.11})$$

with a nodal degree of freedom vector $\{u_1, \theta_1, u_2, \theta_2\}^T$.

The geometric stiffness matrix due to the self weight of a beam element can be expressed as

$$[K_{sw}]_z = q_0 \begin{bmatrix} \frac{3}{5} & \frac{L}{10} & -\frac{3}{5} & 0 \\ \frac{L^2}{30} & \frac{L}{10} & -\frac{L^2}{30} & -\frac{L^2}{30} \\ \text{sym.} & \frac{3}{5L} & 0 & 0 \\ \frac{L^2}{10} & 0 & 0 & \frac{L^2}{10} \end{bmatrix} \quad (\text{A.12})$$

where q_0 is the self weight per unit length of the member.

TORSION ARMS

The local mass and stiffness matrices for a torsion arm were obtained by individually considering a unit displacement on each of the nine DOF at the extremities of the torsion arm. These calculations were conducted by modelling some standard torsion arms using the PC based software package SAP90™.

The stiffness for three different torsion arms was determined using the technique described in Chapter 2. The three torsion arms were identified by their lengths, namely a three meter outrigger, an eight foot outrigger and a twelve foot outrigger. Details of the dimensions, section members and the structural stiffness is presented in the ensuing sections.

THREE METER OUTRIGGER

The dimensions and members sizes are shown for the three meter outrigger in Figure A.3. All dimensions in that figure are in millimeters except for the member sizes which are in imperial units. The resulting stiffness matrix is

$$10^8 \times \begin{bmatrix} 2.85 & 1.26 & 0.167 & -2.85 & -1.26 & -0.167 & -0.249 & 0.494 & 0.494 \\ 1.26 & 0.913 & -0.284 & -1.26 & -0.913 & 0.284 & 0.424 & -0.849 & -0.849 \\ 0.167 & -0.284 & 0.370 & -0.167 & 0.284 & -0.370 & -0.551 & 1.10 & 1.10 \\ -2.85 & -1.26 & -0.167 & 2.85 & 1.26 & 0.167 & 0.249 & -0.494 & -0.494 \\ -1.26 & -0.913 & 0.284 & 1.26 & 0.913 & -0.284 & -0.424 & 0.849 & 0.849 \\ -0.167 & 0.284 & -0.370 & 0.167 & -0.284 & 0.370 & 0.551 & -1.10 & -1.10 \\ -0.249 & 0.424 & -0.551 & 0.249 & -0.424 & 0.551 & 0.833 & -1.64 & -1.64 \\ 0.494 & -0.849 & 1.10 & -0.494 & 0.849 & -1.11 & -1.64 & 3.28 & 3.28 \\ 0.494 & -0.849 & 1.10 & -0.494 & 0.849 & -1.10 & -1.64 & 3.28 & 3.28 \end{bmatrix} \quad (\text{A.13})$$

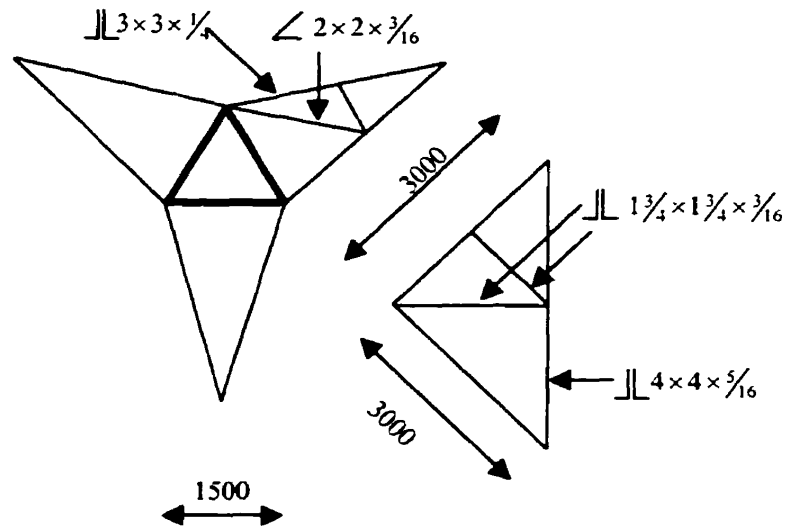


Figure A.3: Three meter outrigger.

EIGHT FOOT OUTRIGGER

The stiffness matrix corresponding to the eight foot outrigger shown in Figure A.4 is presented below. All units in Figure A.4 are imperial.

$$10^8 \times \begin{bmatrix} 3.27 & 1.16 & 0.345 & -3.27 & -1.16 & -0.345 & -0.471 & 0.839 & 1.64 \\ 1.16 & 0.917 & -0.131 & -1.16 & -0.918 & 0.131 & 0.178 & -0.318 & -0.627 \\ 0.345 & -0.131 & 0.167 & -0.345 & 0.131 & -0.167 & -0.227 & 0.402 & 0.787 \\ -3.27 & -1.16 & -0.345 & 3.27 & 1.16 & 0.345 & 0.471 & -0.839 & -1.64 \\ -1.16 & -0.971 & 0.131 & 1.16 & 0.918 & -0.131 & -0.178 & 0.318 & 0.627 \\ -0.345 & 0.131 & -0.167 & 0.345 & -0.131 & 0.167 & 0.227 & -0.402 & -0.787 \\ -0.471 & 0.178 & -0.227 & 0.471 & -0.179 & 0.227 & 0.315 & -0.548 & -1.08 \\ 0.839 & -0.318 & 0.402 & -0.839 & 0.318 & -0.402 & -0.548 & 0.978 & 1.92 \\ 1.64 & -0.627 & 0.787 & -1.64 & 0.627 & -0.787 & -1.08 & 1.92 & 3.76 \end{bmatrix} \quad (\text{A.14})$$

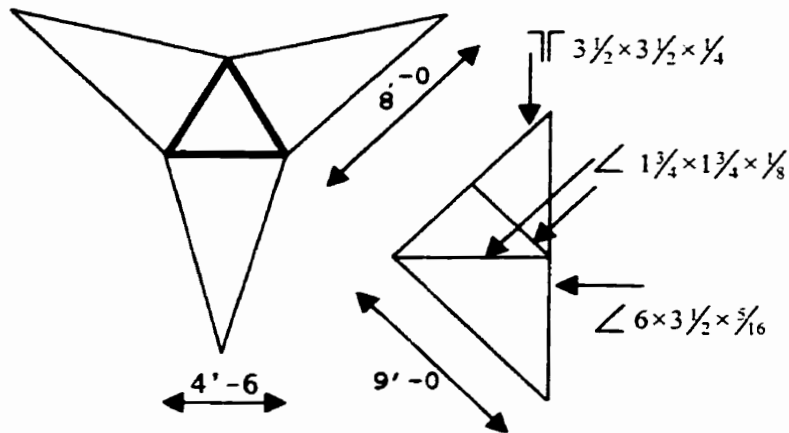


Figure A.4: Eight foot outrigger.

TWELVE FOOT OUTRIGGER

The twelve foot torsion arm has identical dimensions and member sizes with that shown in Figure A.4 with the exception that the 8'-0 section length is replaced by an identical member 12'-0 in length. The resulting stiffness matrix is

$$10^8 \times \begin{bmatrix} 2.97 & 0.866 & 0.125 & -2.97 & -0.866 & -0.125 & -0.171 & -0.458 & 0.891 \\ 0.866 & 0.466 & -0.071 & -0.866 & -0.466 & 0.071 & 0.096 & -0.258 & -0.509 \\ 0.125 & -0.071 & 0.061 & -0.125 & 0.071 & -0.061 & -0.082 & 0.218 & 0.428 \\ -2.97 & -0.866 & -0.125 & 2.97 & 0.866 & 0.125 & 0.171 & 0.458 & -0.891 \\ -0.866 & -0.466 & 0.071 & 0.866 & 0.466 & -0.071 & -0.096 & 0.258 & 0.509 \\ -0.125 & 0.071 & -0.061 & 0.125 & -0.071 & 0.061 & 0.082 & -0.218 & -0.428 \\ -0.171 & 0.096 & -0.082 & 0.171 & -0.096 & 0.082 & 0.114 & -0.298 & -0.584 \\ 0.458 & -0.258 & 0.218 & -0.458 & 0.258 & -0.218 & -0.298 & 0.797 & 1.56 \\ 0.891 & -0.509 & 0.428 & -0.891 & 0.509 & -0.428 & -0.584 & 1.56 & 3.06 \end{bmatrix} \quad (\text{A.15})$$

WTMJ TOWER PROPERTIES

Level	E ($\times 10^6$ psi)	A (in ²)	l (ft)	h (ft)	q (lbs/ft)	Cable Tension at Base (lbs)
1*	24	.938	559	139.4	3.28	28800
2	24	1.13	559	269.4	3.97	18500
3	24	1.13	559	409.4	3.97	25850
4	24	1.13	573.8	549.4	3.97	33100
5	24	3.94	578.9	829.4	13.8	93650

* Bottom Guy

Table A.1: Guy Properties – WTMJ Tower

Segment Number	Segment Weight (lbs/ft)	Segment Length (ft)	Axial Load (Par Model) (lbs)	Axial Load (Cat Model) (lbs)	EI ($\times 10^6$ lbs-in ²)
1	449	30	773417	828793	3.985
2	416	30	760937	816313	3.695
3	354	30	750317	805693	3.149
4	349	30	739847	795223	3.149
5	344	30	708647	761000	3.149
6	344	30	698327	750680	3.149
7	320	30	688727	741080	2.892
8	325	30	678977	731330	2.892
9	354	30	668357	720710	3.149
10	385	30	632717	680685	3.149
11	354	30	622097	670065	2.892
12	342	30	611837	659805	2.892
13	355	30	601187	649155	3.149

14	374	30	544217	586560	3.146
15	374	30	532997	575340	3.146
16	355	30	522347	564690	3.149
17	336	30	512267	554610	2.892
18	319	30	502697	545040	2.646
19	309	30	424577	460114	2.411
20	280	30	416177	451714	2.411
21	281	30	407747	443284	2.411
22	307	30	398537	434074	2.411
23	366	30	387557	423094	3.149
24	429	30	374687	410224	3.695
25	501	30	359657	395194	4.286
26	566	30	342677	378214	4.92
27	651	30	323147	358684	5.598
28	720	30	71747	71747	6.319
29	363	15	63102	63102	2.767
30	267	30	55092	55092	2.079
31	219	30	48522	48522	1.58
32	171	30	43392	43392	1.071
33	138	30	39252	39252	.723
34	205	16	35972	35972	.723
35	483	16	28244	28244	.723
36	684	11	20720	20720	.003
37	583	8	16056	16056	.002
38	491	8	12128	12128	.002
39	406	8	8880	8880	.001
40	330	8	6240	6240	.001
41	261	8	4152	4152	.001
42	201	8	2544	2544	.001
43	148	8	1360	1360	.001

44	103	8	536	536	.001
45	67	8	0	0	.001

Table A.2: Tower Mast Properties – WTMJ Tower